Vol 454|17 July 2008|doi:10.1038/nature07027



LETTERS

# IGFBP-4 is an inhibitor of canonical Wnt signalling required for cardiogenesis

Weidong Zhu[1]*, Ichiro Shiojima[1]*, Yuzuru Ito[2]*, Zhi Li[1], Hiroyuki Ikeda[1], Masashi Yoshida[1], Atsuhiko T. Naito[1], Jun-ichiro Nishi[1], Hiroo Ueno[3], Akihiro Umezawa[4], Tohru Minamino[1], Toshio Nagai[1], Akira Kikuchi[5], Makoto Asashima[2,6,7] & Issei Komuro[1]

**Insulin-like growth-factor-binding proteins (IGFBPs) bind to and modulate the actions of insulin-like growth factors (IGFs)[1]. Although some of the actions of IGFBPs have been reported to be independent of IGFs, the precise mechanisms of IGF-independent actions of IGFBPs are largely unknown[1,2]. Here we report a previously unknown function for IGFBP-4 as a cardiogenic growth factor. IGFBP-4 enhanced cardiomyocyte differentiation *in vitro*, and knockdown of *Igfbp4* attenuated cardiomyogenesis both *in vitro* and *in vivo*. The cardiogenic effect of IGFBP-4 was independent of its IGF-binding activity but was mediated by the inhibitory effect on canonical Wnt signalling. IGFBP-4 physically interacted with a Wnt receptor, Frizzled 8 (Frz8), and a Wnt co-receptor, low-density lipoprotein receptor-related protein 6 (LRP6), and inhibited the binding of Wnt3A to Frz8 and LRP6. Although IGF-independent, the cardiogenic effect of IGFBP-4 was attenuated by IGFs through IGFBP-4 sequestration. IGFBP-4 is therefore an inhibitor of the canonical Wnt signalling required for cardiogenesis and provides a molecular link between IGF signalling and Wnt signalling.**

The heart is the first organ to form during embryogenesis, and abnormalities in this process result in congenital heart diseases, the most common cause of birth defects in humans[3]. Molecules that mediate cardiogenesis are of particular interest because of their potential use for cardiac regeneration[4,5]. Previous studies have shown that soluble growth factors such as bone morphogenetic proteins (BMPs), fibroblast growth factors (FGFs), Wnts and Wnt inhibitors mediate the tissue interactions that are crucial for cardiomyocyte specification[3,4]. We proposed that there might be additional soluble factors that modulate cardiac development and/or cardiomyocyte differentiation.

P19CL6 cells differentiate into cardiomyocytes with high efficiency in the presence of 1% dimethylsulphoxide (DMSO)[6]. We cultured P19CL6 cells with culture media conditioned by various cell types in the absence of DMSO, and screened the cardiogenic activity of the conditioned media. The extent of cardiomyocyte differentiation was assessed by the immunostaining with MF20 monoclonal antibody that recognizes sarcomeric myosin heavy chain (MHC). Among the several cell types tested, culture media conditioned by a murine stromal cell line OP9 induced cardiomyocyte differentiation of P19CL6 cells without DMSO treatment (Fig. 1a, left and middle panels). Increased MF20-positive area was accompanied by the induction of cardiac marker genes such as *αMHC*, *Nkx2.5* and *GATA-4*, and by the increased protein levels of cardiac troponin T (cTnT) (Fig. 1a, right panel). In contrast, culture media conditioned by COS7 cells, mouse embryonic fibroblasts, NIH3T3 cells, HeLa cells, END2 cells (visceral endoderm-like cells), neonatal rat cardiomyocytes and neonatal rat cardiac fibroblasts did not induce cardiomyocyte differentiation of P19CL6 cells in the absence of DMSO (Fig. 1a and data not shown). From these observations, we postulated that OP9 cells secrete one or more cardiogenic growth factors.

To identify an OP9-derived cardiogenic factor, complementary DNA clones isolated by a signal sequence trap method from an OP9 cell cDNA library[7] were tested for their cardiogenic activities by transient transfection. When available, recombinant proteins were also used to confirm the results. Among candidate factors tested, IGFBP-4 induced cardiomyocyte differentiation of P19CL6 cells, as demonstrated by the increase in MF20-positive area and the induction of cardiac markers (Fig. 1b). We also cultured P19CL6 cells with OP9-conditioned media pretreated with an anti-IGFBP-4 neutralizing antibody. The application of an anti-IGFBP-4 neutralizing antibody attenuated the efficiency of cardiomyocyte differentiation induced by OP9-conditioned media (Fig. 1c). These findings strongly suggest that IGFBP-4 is a cardiogenic factor secreted from OP9 cells.

Because IGFBPs have been characterized as molecules that bind to and modulate the actions of IGFs, we tested whether IGFBP-4 promotes cardiogenesis by either enhancing or inhibiting the actions of IGFs. We first treated P19CL6 cells with a combination of anti-IGF-I and IGF-II-neutralizing antibodies or a neutralizing antibody against type-I IGF receptor. If IGFBP-4 induces cardiomyocyte differentiation by inhibiting IGF signalling, treatment with these antibodies should induce cardiomyocyte differentiation and/or enhance the cardiogenic effects of IGFBP-4. In contrast, if IGFBP-4 promotes cardiogenesis by enhancing IGF signalling, treatment with these antibodies should attenuate IGFBP-4-mediated cardiogenesis. However, treatment with these antibodies did not affect the efficiency of IGFBP-4-induced cardiomyocyte differentiation (Fig. 1d and data not shown). Treatment of P19CL6 cells with IGF-I and IGF-II also did not induce cardiomyocyte differentiation (data not shown). Furthermore, treatment with an IGFBP-4 mutant (IGFBP-4-H74P; His 74 replaced by Pro)[8] that is unable to bind IGFs induced cardiomyocyte differentiation of P19CL6 cells even more efficiently than wild-type IGFBP-4 (Fig. 1e). This is presumably due to the sequestration of wild-type IGFBP-4 but not mutant IGFBP-4-H74P by endogenous IGFs. In agreement with this idea, exogenous IGFs attenuated wild-type IGFBP-4-induced but not IGFBP-4-H74P-induced cardiogenesis (Fig. 1f). Taken together, these observations indicate

[1]Department of Cardiovascular Science and Medicine, Chiba University Graduate School of Medicine, Chiba 260-8670, Japan. [2]ICORP Organ Regeneration Project, Japan Science and Technology Agency (JST), Tokyo 153-8902, Japan. [3]Institute of Stem Cell Biology and Regenerative Medicine, Stanford University School of Medicine, Stanford, California 94305, USA. [4]Department of Reproductive Biology, National Institute for Child Health and Development, Tokyo 157-8535, Japan. [5]Department of Biochemistry, Graduate School of Biomedical Sciences, Hiroshima University, Hiroshima 734-8551, Japan. [6]Department of Life Sciences (Biology), Graduate School of Arts and Science, The University of Tokyo, Tokyo 153-8902, Japan. [7]National Institute of Advanced Industrial Sciences and Technology (AIST), Ibaraki 305-8562, Japan.
*These authors contributed equally to this work.

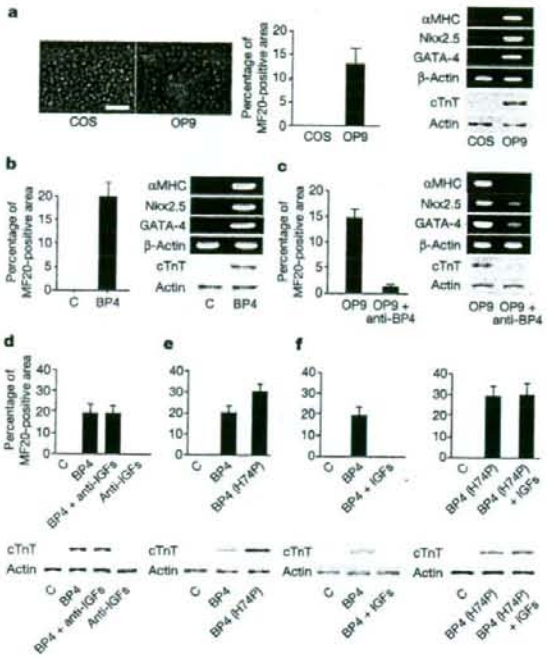


**Figure 1 | IGFBP-4 promotes cardiomyocyte differentiation in an IGF-independent manner.** **a**, Culture media conditioned by OP9 cells but not by COS7 cells induced cardiomyocyte differentiation of P19CL6 cells as assessed by MF20-positive area, cardiac marker-gene expression and cTnT protein expression. Scale bar, 100 μm. Error bars show s.d. **b**, Treatment with IGFBP-4 (1 μg ml$^{-1}$) induced cardiomyocyte differentiation of P19CL6 cells in the absence of DMSO. Error bars show s.d. **c**, Treatment with a neutralizing antibody against IGFBP-4 (anti-BP4; 40 μg ml$^{-1}$) attenuated cardiomyocyte differentiation of P19CL6 cells induced by OP9-conditioned media. Error bars show s.d. **d**, Treatment with neutralizing antibodies against IGF-I and IGF-II (anti-IGFs; 5 μg ml$^{-1}$ each) had no effect on IGFBP-4-induced cardiomyocyte differentiation of P19CL6 cells. Error bars show s.d. **e**, Mutant IGFBP-4 (BP4(H74P)) that is incapable of binding to IGFs retained cardiomyogenic activity. Error bars show s.d. **f**, IGFs (100 ng ml$^{-1}$ each) attenuated wild-type IGFBP-4-induced but not mutant IGFBP-4-H74P-induced cardiomyocyte differentiation of P19CL6 cells. Error bars show s.d.

that IGFBP-4 induces cardiomyocyte differentiation in an IGF-independent fashion.

To explore further the mechanisms by which IGFBP-4 induces cardiomyogenesis, we tested the hypothesis that IGFBP-4 might modulate the signals activated by other secreted factors implicated in cardiogenesis. It has been shown that canonical Wnt signalling is crucial in cardiomyocyte differentiation[3,4]. In P19CL6 cells, Wnt3A treatment activated β-catenin-dependent transcription of the TOPFLASH reporter gene, and this activation was attenuated by IGFBP-4 (Fig. 2a). Wnt/β-catenin signalling is transduced by the cell-surface receptor complex consisting of Frizzled and low-density-lipoprotein receptor (LDLR)-related protein 5/6 (LRP5/6)[9] and IGFBP-4 attenuated TOPFLASH activity enhanced by the expression of LRP6 or Frizzled 8 (Frz8) (Fig. 2a). As a control, IGFBP-4 did not alter BMP-mediated activation of a BMP-responsive reporter BRE–luc (Supplementary Fig. 1b). These findings suggest that IGFBP-4 is a specific inhibitor of the canonical Wnt pathway. To examine this possibility *in vivo*, we performed axis duplication assays in *Xenopus* embryos. Injection of *Xwnt8* or *Lrp6* mRNA caused secondary axis formation, and injection of *Xenopus IGFBP-4* (*XIGFBP-4*) mRNA alone had minimal effects on axis formation. However, Xwnt8-induced or LRP6-induced secondary axis formation was efficiently blocked by coexpression of XIGFBP-4 (Fig. 2b, c), indicating that IGFBP-4 inhibits canonical Wnt signalling *in vivo*. To explore the mechanisms of Wnt inhibition by IGFBP-4, *Xenopus* animal cap assays and TOPFLASH reporter gene assays were performed. In animal cap assays, IGFBP-4 inhibited LRP6-induced but not β-catenin-induced Wnt-target gene expression (Supplementary Fig. 1c). Similarly, IGFBP-4 attenuated Wnt3A-induced or LRP6-induced TOPFLASH activity but did not alter Dishevelled-1 (Dvl-1)-induced, LiCl-induced or β-catenin-induced TOPFLASH activity (Supplementary Fig. 1d, e). These findings suggest that IGFBP-4 inhibits canonical Wnt signalling at the level of cell-surface receptors. To examine whether IGFBP-4 antagonizes Wnt signalling via direct physical interaction with LRP5/6 or Frizzled, we produced conditioned media containing the Myc-tagged extracellular portion of LRP6 (LRP6N–Myc), the Myc-tagged cysteine-rich domain (CRD) of Frz8 (Frz8CRD–Myc), and V5-tagged IGFBP-4 (IGFBP-4–V5). Immunoprecipitation (IP)/western blot experiments revealed that IGFBP-4 interacted with LRP6N (Fig. 2d) and Frz8CRD (Fig. 2e). A liquid-phase binding assay with $^{125}$I-labelled IGFBP-4 and conditioned media containing LRP6N–Myc or Frz8CRD–Myc demonstrated that the interaction between IGFBP-4 and LRP6N or Frz8CRD was specific and saturable (Fig. 2f, g). A Scatchard plot analysis revealed two binding sites with different binding affinities for LRP6N (Fig. 2f, inset) and a single binding site for Frz8CRD (Fig. 2g, inset). A similar binding assay with $^{125}$I-labelled Wnt3A demonstrated that IGFBP-4 inhibited Wnt3A binding to LRP6N (Fig. 2h) and Frz8CRD (Fig. 2i), and a Lineweaver–Burk plot revealed that IGFBP-4 was a competitive inhibitor of the binding of Wnt3A to Frz8CDR (Supplementary Fig. 2a). IP/western blot analyses with various deletion mutants of LRP6 and IGFBP-4 revealed that IGFBP-4 interacted with multiple domains of LRP6 and that the carboxy-terminal thyroglobulin domain of IGFBP-4 was required for IGFBP-4 binding to LRP6 or Frz8CRD (Supplementary Fig. 2b–f). It has been shown that inhibition of canonical Wnt signalling promotes cardiomyocyte differentiation in embryonic stem (ES) cells and in chick, *Xenopus* and zebrafish embryos[4,10,11]. These results therefore collectively suggest that IGFBP-4 promotes cardiogenesis by antagonizing the Wnt/β-catenin pathway through direct interactions with Frizzled and LRP5/6.

Next we investigated the role of endogenous IGFBP-4 in P19CL6 cell differentiation into cardiomyocytes. Reverse transcriptase-mediated polymerase chain reaction (RT–PCR) analysis revealed that the expression of *Igfbp4* was upregulated during DMSO-induced P19CL6 cell differentiation (Fig. 3a). Expression of *Igfbp3* and *Igfbp5* was also upregulated in the early and the late phases of differentiation, respectively. Expression of *Igfbp2* was not altered, and that of *Igfbp1* or *Igfbp6* was not detected. When IGFBP-4 was knocked down by two different small interfering RNA (siRNA) constructs, DMSO-induced cardiomyocyte differentiation was inhibited in both cases (Fig. 3b). In contrast, knockdown of *Igfbp3* or *Igfbp5* did not inhibit DMSO-induced cardiomyocyte differentiation (Fig. 3b, right panel). Treatment with an anti-IGFBP-4 neutralizing antibody also blocked DMSO-induced cardiomyocyte differentiation (Fig. 3c). Secretion of endogenous IGFBP-4 is therefore required for the differentiation of P19CL6 cells into cardiomyocytes. Immunostaining for IGFBP-4 revealed that cardiac myocytes were surrounded by the IGFBP-4-positive cells, suggesting that a paracrine effect of IGFBP-4 on cardiomyocyte differentiation is predominant (Fig. 3d). Essentially the same results were obtained in ES cells (Supplementary Fig. 3d–g). To investigate whether IGFBP-4 promotes the differentiation of P19CL6 cells into cardiomyocytes by the inhibition of the canonical Wnt pathway, we expressed dominant-negative LRP6 (LRP6N) in P19CL6 cells. Expression of LRP6N enhanced cardiomyocyte differentiation of P19CL6 cells and reversed the inhibitory effect of *Igfbp4*

knockdown on cardiomyogenesis (Fig. 3e). These observations suggest that endogenous IGFBP-4 is required for cardiomyocyte differentiation of P19CL6 cells and ES cells, and that the cardiogenic effect of IGFBP-4 is mediated by its inhibitory effect on Wnt/β-catenin signalling.

The role of endogenous IGFBP-4 in cardiac development *in vivo* was also examined with *Xenopus* embryos. Whole-mount *in situ* hybridization analysis revealed that strong expression of *XIGFBP-4* was detected at stage 38 in the anterior part of the liver adjacent to the heart (Fig. 4a). Knockdown of *XIGFBP-4* by two different morpholino (MO) constructs resulted in cardiac defects, with more than 70% of the embryos having a small heart or no heart (Fig. 4b). The specificity of MO was confirmed by the observation that simultaneous injection of MO-resistant *XIGFBP-4* cDNA rescued the MO-induced cardiac defects (Fig. 4b, Supplementary Fig. 4c). Coexpression of IGF-binding-defective XIGFBP-4 mutant (XIGFBP-4-H74P) or dominant-negative LRP6 (LRP6N) also rescued the cardiac defects induced by *XIGFBP-4* knockdown (Fig. 4b), whereas overexpression of Xwnt8 in the heart-forming region resulted in cardiac defects similar to those induced by *XIGFBP-4* knockdown (Supplementary Fig. 4d–f), supporting the notion that the cardiogenic effect of IGFBP-4 is independent of IGFs but is mediated by inhibition of the Wnt/β-catenin pathway. The temporal profile of cardiac defects induced by *XIGFBP-4* knockdown was also examined by *in situ* hybridization with *cardiac troponin I* (*cTnI*) (Fig. 4c). At stage 34, morphology of the heart was comparable between control embryos and MO-injected embryos. However, at stage 38, when *XIGFBP-4* starts to be expressed in the anterior part of the liver, the expression of *cTnI* was markedly attenuated in MO-injected embryos; expression of *cTnI* was diminished and no heart-like structure was observed at stage 42. Thus, the heart is initially formed but its subsequent growth is perturbed in the absence of XIGFBP-4, suggesting that IGFBP-4

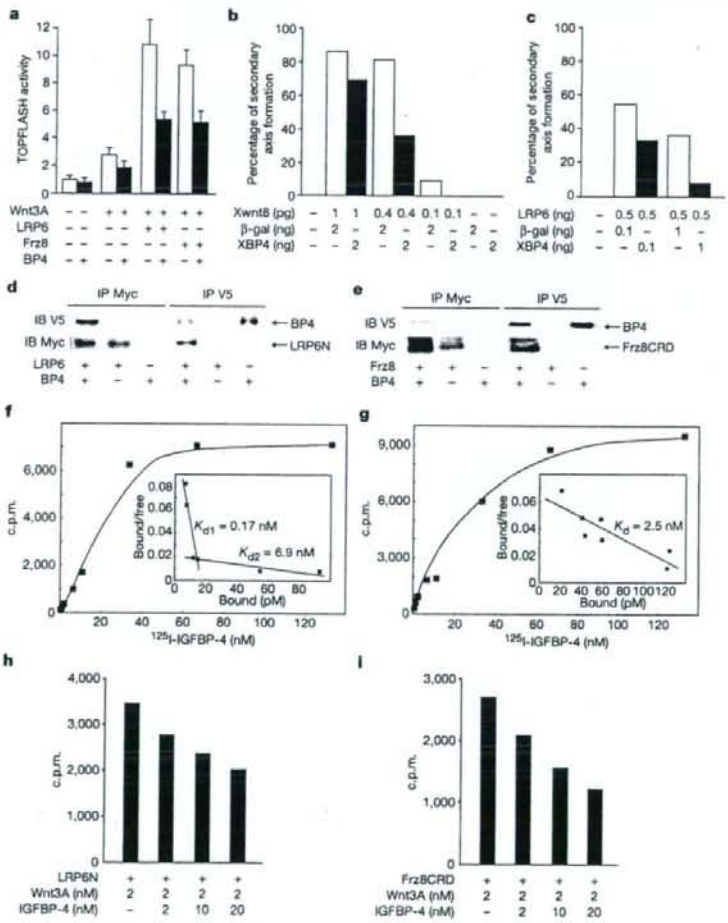


**Figure 2 | IGFBP-4 inhibits Wnt/β-catenin signalling through direct interactions with Wnt receptors.** **a**, IGFBP-4 attenuated β-catenin-dependent transcription in P19CL6 cells. P19CL6 cells were transfected with TOPFLASH reporter gene and expression vectors for LRP6 or Frz8, and then treated with Wnt3A or Wnt3A plus IGFBP-4; luciferase activities were then measured. Error bars show s.d. **b**, XIGFBP-4 (XBP4) inhibited Xwnt8-induced secondary-axis formation in *Xenopus* embryos ($n = 20$ for each group). **c**, IGFBP-4 inhibited LRP6-induced secondary-axis formation in *Xenopus* embryos ($n = 30$ for each group). **d**, **e**, IGFBP-4 interacted directly with LRP6N (**d**) and Frz8CRD (**e**). IB, immunoblotting; IP, immunoprecipitation. **f**, A binding assay between $^{125}$I-labelled IGFBP-4 and LRP6N. The inset is a Scatchard plot showing two binding sites with different binding affinities. **g**, A binding assay between $^{125}$I-labelled IGFBP-4 and Frz8CRD. The inset is a Scatchard plot showing a single binding site. **h**, **i**, IGFBP-4 inhibited Wnt3A binding to LRP6N (**h**) or Frz8CRD (**i**). $^{125}$I-labelled Wnt3A binding to LRP6N or Frz8CRD was assessed in the presence of increasing amounts of IGFBP-4.

promotes cardiogenesis by maintaining the proliferation and/or survival of embryonic cardiomyocytes.

It has been shown that canonical Wnt signals inhibit cardiogenesis in chick and frog embryos, and that Wnt antagonists such as Dkk1 and Crescent secreted from the anterior endoderm or the organizer region counteract the Wnt-mediated inhibitory signals and induce cardiogenesis in the anterior lateral mesoderm[4]. However, IGFBP-4-mediated Wnt inhibition is required at later stages of development, when the heart is already formed at the ventral portion and starts to grow and remodel to maintain embryonic circulation. It has been shown that Wnt/β-catenin signalling has time-dependent effects on cardiogenesis in ES cells: canonical Wnt signalling in the early phase of ES-cell differentiation promotes cardiomyogenesis, whereas it inhibits cardiomyocyte differentiation in the late phase[10–12]. In agreement with this notion, IGFBP-4 promoted cardiomyocyte differentiation of ES cells only when IGFBP-4 was applied in the late phase after embryoid body formation (Supplementary Fig. 3a–c). Similar time-dependent effects of Wnt/β-catenin signalling on cardiogenesis has been shown in zebrafish embryos[11]. Moreover, several recent reports suggest that Wnt/β-catenin signalling is a positive regulator of cardiac progenitor-cell proliferation in the secondary heart field[13]. It therefore seems that canonical Wnt signalling has divergent effects on cardiogenesis at multiple stages of development: first, canonical Wnt signalling promotes cardiogenesis at the time of gastrulation or mesoderm specification; second, it inhibits cardiogenesis at the time when cardiac mesoderm is specified in the anterior lateral mesoderm; third, it promotes the expansion of cardiac progenitors in the secondary heart field; and fourth, it inhibits cardiogenesis at later stages when the embryonic heart is growing. It is interesting to note that IGFBP-4 is expressed predominantly in the liver. Mouse IGFBP-4 is

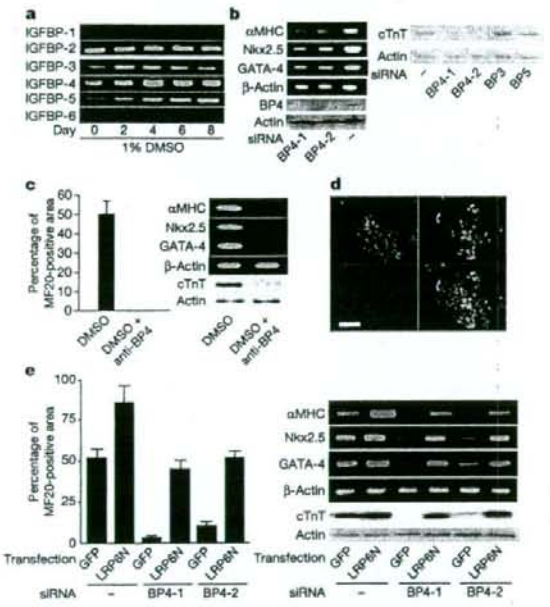


**Figure 3 | IGFBP-4 is required for the differentiation of P19CL6 cells into cardiomyocytes.** **a**, Expression analysis of IGFBP family members by RT–PCR during DMSO-induced cardiomyocyte differentiation of P19CL6 cells (from day 0 to day 8). **b**, Left: knockdown of *Igfbp4* in P19CL6 cells attenuated cardiac marker expression in response to treatment with DMSO. BP4-1 and BP4-2 represent two different siRNAs for IGFBP-4. Right: knockdown of *Igfbp3* or *Igfbp5* had no effect on cTnT expression in response to DMSO treatment. **c**, Treatment with a neutralizing antibody against IGFBP-4 (anti-BP4; 40 μg ml$^{-1}$) attenuated DMSO-induced cardiomyocyte differentiation of P19CL6 cells. Error bars show s.d. **d**, IGFBP-4 immunostaining during DMSO-induced differentiation of P19CL6 cells stably transfected with αMHC–green fluorescent protein (GFP) reporter gene. Top left, IGFBP-4 staining (red); top right, GFP expression representing differentiated cardiomyocytes; bottom left, nuclear staining with DAPI (4′,6-diamidino-2-phenylindole); bottom right, a merged picture. Scale bar, 100 μm. **e**, Attenuated cardiomyocyte differentiation of P19CL6 cells by *Igfbp4* knockdown was rescued by inhibiting Wnt/β-catenin signalling. Control and *Igfbp4*-knocked-down P19CL6 cells were transfected with an expression vector for GFP or LRP6N (a dominant-negative form of LRP6) and induced to differentiate into cardiomyocytes by treatment with DMSO. LRP6N overexpression rescued the attenuated cardiomyocyte differentiation induced by *Igfbp4* knockdown as assessed by MF20-positive area (left panel), cardiac marker-gene expression and cTnT protein expression (right panel). Error bars show s.d.

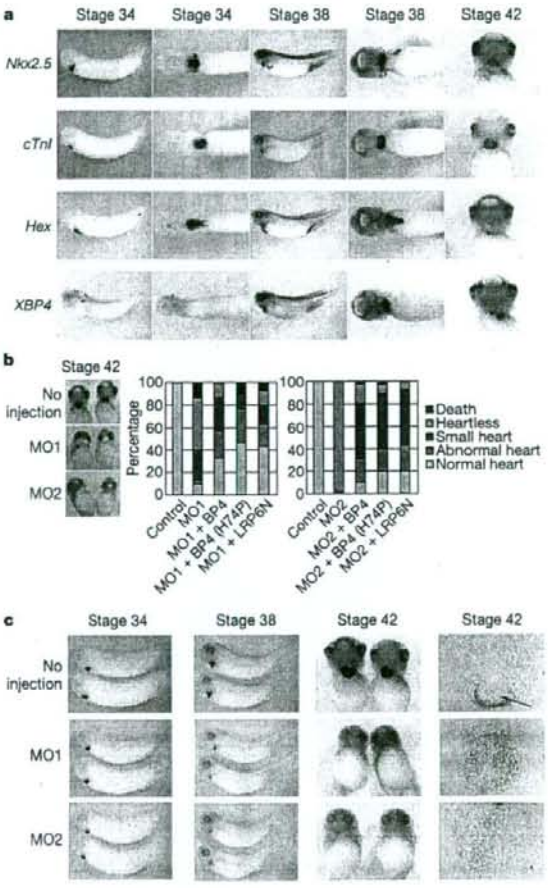


**Figure 4 | IGFBP-4 is required for the maturation of the heart in *Xenopus* embryos.** **a**, *In situ* hybridization analysis of *Nkx2.5* (an early cardiac marker), *cTnI* (a mature cardiac marker), *Hex* (a liver marker), and *XIGFBP-4* (*XBP4*) mRNA expression at stages 34, 38 and 42. **b**, Knockdown of *XIGFBP-4* by two different morpholinos (MO1 and MO2) resulted in severe cardiac defects as assessed by *cTnI in situ* hybridization at stage 42 (left). These cardiac defects were rescued by simultaneous injection of MO-resistant wild-type XIGFBP-4, mutant XIGFBP-4-H74P (BP4(H74P) and LRP6N ($n = 30$ for each group). **c**, Temporal profile of cardiac defects induced by *XIGFBP-4* knockdown. Morphology of the heart as assessed by cTnI *in situ* hybridization was almost normal at stage 34 but was severely perturbed at stages 38 and 42. The right column shows sections of control and MO-injected embryos. The arrow indicates the heart in control embryos. No heart-like structure was observed in MO-injected embryos.

also strongly expressed in the tissues adjacent to the heart such as pharyngeal arches and liver bud at embryonic day (E)9.5 (Supplementary Fig. 3h). These observations and the results of IGFBP-4 immunostaining in P19CL6 cells and ES cells suggest that IGFBP-4 promotes cardiogenesis in a paracrine fashion. Together with a previous report showing that cardiac mesoderm secretes FGFs and induces liver progenitors in the ventral endoderm[14], these observations suggest that there exist reciprocal paracrine signals between the heart and the liver that coordinately promote the development of each other.

IGFBPs are composed of six members, IGFBP-1 to IGFBP-6. Reporter gene assays and β-catenin stabilization assays revealed that IGFBP-4 was the most potent canonical Wnt inhibitor and that IGFBP-1, IGFBP-2 and IGFBP-6 also showed modest activity in Wnt inhibition, whereas IGFBP-3 and IGFBP-5 had no such activity (Supplementary Fig. 5a–c). In agreement with this, IP/western blot analyses demonstrated that IGFBP-1, IGFBP-2, IGFBP-4 and IGFBP-6 but not IGFBP-3 or IGFBP-5 interacted with LRP6 or Frz8CRD (Supplementary Fig. 5d, e). Thus, the lack of cardiac phenotypes in IGFBP-4-null mice or IGFBP-3/IGFBP-4/IGFBP-5 triple knockout mice[15] may be due to genetic redundancies between IGFBP-4 and other IGFBPs such as IGFBP-1, IGFBP-2 and/or IGFBP-6.

The identification of IGFBP-4 as an inhibitor of Wnt/β-catenin signalling may also have some implications for cancer biology[16]. It was shown that treatment with IGFBP-4 reduces cell proliferation in some cancer cell lines *in vitro*, and that overexpression of IGFBP-4 attenuates the growth of prostate cancer *in vivo*. Decreased serum levels of IGFBP-4 are associated with the risk of breast cancer. Because the activation of Wnt signalling is implicated in several forms of malignant tumours[17,18], it is possible that the inhibitory effect of IGFBP-4 on cell proliferation is mediated in part by the inhibition of canonical Wnt signalling.

## METHODS SUMMARY

**Cell culture.** P19CL6 cells and ES cells were cultured and induced to differentiate into cardiomyocytes essentially as described[6,18]. P19CL6 cells (2,000 cells per 35-mm dish) were treated with various conditioned media for screening of their cardiogenic activities. For siRNA-mediated knockdown, pSIREN-RetroQ vectors (Clontech) ligated with double-stranded oligonucleotides were transfected into P19CL6 cells or ES cells, and puromycin-resistant clones were selected.

**IP/western blot analyses and binding assays.** Conditioned media for IP/western blot analyses were produced by using 293 cells. Binding reactions were performed overnight at 4 °C. $^{125}$I-labelling of IGFBP-4 and Wnt3A was performed with IODO-BEADS Iodination Reagent (Pierce). A liquid-phase binding assay was performed essentially as described[19].

***Xenopus* experiments.** Axis duplication assays, animal cap assays, and *in situ* hybridization analyses in *Xenopus* were performed essentially as described[20]. Electroporation of mRNA was performed at stage 28 essentially as described[21].

**Full Methods** and any associated references are available in the online version of the paper at www.nature.com/nature.

**Received 22 August 2007; accepted 24 April 2008.**
**Published online 4 June 2008.**

1. Firth, S. M. & Baxter, R. C. Cellular actions of the insulin-like growth factor binding proteins. *Endocr. Rev.* 23, 824–854 (2002).
2. Mohan, S. & Baylink, D. J. IGF-binding proteins are multifunctional and act via IGF-dependent and -independent mechanisms. *J. Endocrinol.* 175, 19–31 (2002).
3. Olson, E. N. & Schneider, M. D. Sizing up the heart: development redux in disease. *Genes Dev.* 17, 1937–1956 (2003).
4. Foley, A. & Mercola, M. Heart induction: embryology to cardiomyocyte regeneration. *Trends Cardiovasc. Med.* 14, 121–125 (2004).
5. Leri, A., Kajstura, J. & Anversa, P. Cardiac stem cells and mechanisms of myocardial regeneration. *Physiol. Rev.* 85, 1373–1416 (2005).
6. Monzen, K. *et al.* Bone morphogenetic proteins induce cardiomyocyte differentiation through the mitogen-activated protein kinase kinase kinase TAK1 and cardiac transcription factors Csx/Nkx-2.5 and GATA-4. *Mol. Cell. Biol.* 19, 7096–7105 (1999).
7. Ueno, H. *et al.* A stromal cell-derived membrane protein that supports hematopoietic stem cells. *Nature Immunol.* 4, 457–463 (2003).
8. Qin, X., Strong, D. D., Baylink, D. J. & Mohan, S. Structure–function analysis of the human insulin-like growth factor binding protein-4. *J. Biol. Chem.* 273, 23509–23516 (1998).
9. Moon, R. T., Kohn, A. D., De Ferrari, G. V. & Kaykas, A. WNT and β-catenin signalling: diseases and therapies. *Nature Rev. Genet.* 5, 691–701 (2004).
10. Naito, A. T. *et al.* Developmental stage-specific biphasic roles of Wnt/β-catenin signaling in cardiomyogenesis and hematopoiesis. *Proc. Natl Acad. Sci. USA* 103, 19812–19817 (2006).
11. Ueno, S. *et al.* Biphasic role for Wnt/β-catenin signaling in cardiac specification in zebrafish and embryonic stem cells. *Proc. Natl Acad. Sci. USA* 104, 9685–9690 (2007).
12. Liu, Y. *et al.* Sox17 is essential for the specification of cardiac mesoderm in embryonic stem cells. *Proc. Natl Acad. Sci. USA* 104, 3859–3864 (2007).
13. Cohen, E. D., Tian, Y. & Morrisey, E. E. Wnt signaling: an essential regulator of cardiovascular differentiation, morphogenesis and progenitor self-renewal. *Development* 135, 789–798 (2008).
14. Jung, J., Zheng, M., Goldfarb, M. & Zaret, K. S. Initiation of mammalian liver development from endoderm by fibroblast growth factors. *Science* 284, 1998–2003 (1999).
15. Ning, Y. *et al.* Diminished growth and enhanced glucose metabolism in triple knockout mice containing mutations of insulin-like growth factor binding protein-3, -4, and -5. *Mol. Endocrinol.* 20, 2173–2186 (2006).
16. Durai, R. *et al.* Biology of insulin-like growth factor binding protein-4 and its role in cancer. *Int. J. Oncol.* 28, 1317–1325 (2006).
17. Logan, C. Y. & Nusse, R. The Wnt signaling pathway in development and disease. *Annu. Rev. Cell Dev. Biol.* 20, 781–810 (2004).
18. Clevers, H. Wnt/β-catenin signaling in development and disease. *Cell* 127, 469–480 (2006).
19. Semenov, M. V. *et al.* Head inducer Dickkopf-1 is a ligand for Wnt coreceptor LRP6. *Curr. Biol.* 11, 951–961 (2001).
20. Kobayashi, H. *et al.* Novel Daple-like protein positively regulates both the Wnt/β-catenin pathway and the Wnt/JNK pathway in *Xenopus*. *Mech. Dev.* 122, 1138–1153 (2005).
21. Sasagawa, S., Takabatake, T., Takabatake, Y., Muramatsu, T. & Takeshima, K. Improved mRNA electroporation method for *Xenopus* neurula embryos. *Genesis* 33, 81–85 (2002).

**Supplementary Information** is linked to the online version of the paper at www.nature.com/nature.

**Acknowledgements** We thank E. Fujita, R. Kobayashi and Y. Ishiyama for technical support; T. Yamauchi and K. Ueki for advice on binding assays; and Y. Onuma and S. Takahashi for advice on *Xenopus* electroporation. This work was supported by grants from the Ministry of Education, Culture, Sports, Science and Technology (MEXT), the Ministry of Health, Labour, and Welfare, and the New Energy and Industrial Technology Development Organization (NEDO).

**Author Contributions** W.Z., I.S. and Y.I. contributed equally to this work. I.K. designed and supervised the research. W.Z., I.S., Y.I., Z.L., H.I., M.Y. and A.T.N. performed experiments. J.N., H.U., A.U., T.M., T.N., A.K. and M.A. contributed new reagents and/or analytical tools. W.Z., I.S., Y.I., A.K. and I.K. analysed data. W.Z., I.S., Y.I. and I.K. prepared the manuscript.

**Author Information** Reprints and permissions information is available at www.nature.com/reprints. Correspondence and requests for materials should be addressed to I.K. (komuro-tky@umin.ac.jp).

## METHODS

**Plasmids and reagents.** cDNA clones encoding mouse IGFBPs and *Xenopus* IGFBP-4 were purchased from Open Biosystems. XIGFBP-4-H74P mutant was generated with a QuickChange Site-Directed Mutagenesis kit (Stratagene). His-tagged human wild-type IGFBP-4 and mutant IGFBP-4-H74P (vectors provided by X. Qin)[8] were produced and purified with HisTrap HP Kit (Amersham). Full-length Frz8, Frz8CRD and LRP6N were provided by X. He[22,23]. Full-length LRP6, membrane-bound forms of LRP6 deletion mutants, and Dkk1 were from C. Niehrs[24]. pXwnt8 and pCSKA-Xwnt8 were from J. Christian[25]. pCS2–β-catenin was from D. Kimelman[26]. αMHC–GFP was from B. Fleischmann[27]. BRE–luc was from P. ten Dijke[28]. pCGN-Dvl-1 was described previously[29]. Soluble forms of LRP6 deletion mutants and probes for *in situ* hybridization analysis (Nkx2.5, cTnI and Hex) were generated by PCR. IGFBP-4, Wnt3A, IGF-I, IGF-II and BMP2 were from R&D. Neutralizing antibodies were from R&D (anti-IGFBP-4), Sigma (anti-IGF-I and anti-IGF-II), and Oncogene (anti-type-I IGF receptor). The antibodies used for immunoprecipitation, western blotting and immunostaining were from Invitrogen (anti-Myc, anti-V5), Santa Cruz (anti-cTnT, anti-IGFBP-4, anti-topoisomerase I (TOPO-I)), Sigma (anti-β-actin, anti-β-catenin, anti-FLAG (M2)) and Developmental Studies Hybridoma Bank (anti-sarcomeric myosin heavy chain (MF20)).

**Cell culture experiments.** P19CL6 cells and ES cells were cultured and induced to differentiate into cardiomyocytes essentially as described[8,10]. P19CL6 cells (2,000 cells per 35-mm dish) were treated with various conditioned media for screening of their cardiogenic activities. P19CL6 cells or ES cells stably transfected with αMHC promoter driven–GFP were generated by transfection of αMHC–GFP plasmid into P19CL6 cells or ht7 ES cells followed by G418 selection. Luciferase reporter gene assays, western blot analyses, immunostaining and RT–PCR were performed as described[10]. Reporter gene assays were repeated at least three times. PCR primers and PCR conditions are listed in Supplementary Table 1. For siRNA-mediated knockdown, siRNAs were expressed with pSIREN-RetroQ vector (Clontech). Oligonucleotide sequences used are listed in Supplementary Table 2. pSIREN-RetroQ vectors ligated with double-stranded oligonucleotides were transfected into P19CL6 cells or ES cells, and puromycin-resistant clones were isolated and expanded. For β-catenin stabilization assays, nuclear extracts of L cells were prepared with NE-PER Nuclear and Cytoplasmic Extraction Reagents (Pierce). Data are shown as means and s.d.

**IP/western blot analyses and binding assays.** Conditioned media for IP/western blot analyses containing full-length or various deletion mutants of IGFBPs, LRP6, Frz8CRD and Dkk1 were produced with 293 cells. Binding reactions were performed overnight at 4 °C. Immunoprecipitation was performed with Protein G–Sepharose 4 Fast Flow (Amersham). $^{125}$I-labelling of IGFBP-4 and Wnt3A was performed with IODO-BEADS Iodination Reagent (Pierce). A liquid-phase binding assay was performed essentially as described[19]. In brief, conditioned media containing LRP6N–Myc or Frz8CRD–Myc were mixed with various concentrations of $^{125}$I-labelled IGFBP-4 and incubated overnight at 4 °C. LRP6N–Myc or Frz8CRD–Myc was immunoprecipitated and the radioactivity of bound IGFBP-4 was measured after extensive washing of the Protein G–Sepharose beads. For a competitive binding assay, conditioned media containing LRP6N–Myc or Frz8CRD–Myc were mixed with $^{125}$I-labelled Wnt3A and unlabelled IGFBP-4, and incubated overnight at 4 °C. LRP6N–Myc or Frz8CRD–Myc was then immunoprecipitated and the radioactivity of bound Wnt3A was measured.

***Xenopus* experiments and mouse *in situ* hybridization analysis.** Axis duplication assays, animal cap assays and *in situ* hybridization analyses in *Xenopus* were performed essentially as described[20]. Two independent cDNAs for *XIGFBP-4*, presumably resulting from pseudotetraploid genomes, were identified by 5′ rapid amplification of cDNA ends (Supplementary Fig. 4a). Two different MOs targeting both of these two IGFBP-4 transcripts were designed (Gene Tools) (Supplementary Fig. 4a and Supplementary Table 2). MO-sensitive *XIGFBP-4* cDNA including a 41-base-pair 5′-untranslated region (UTR) was generated by PCR. MO-resistant *XIGFBP-4* cDNA (wild-type and H74P mutant) was generated by introducing five silent mutations in the MO1 target sequence and excluding the 5′-UTR (Supplementary Fig. 4a). To determine the specificity of MOs, MO-sensitive or MO-resistant *XIGFBP-4–myc* mRNA was injected into *Xenopus* embryos with or without MOs, and protein/mRNA expression was analysed. PCR primers and PCR conditions are listed in Supplementary Table 1. MOs and plasmid DNAs were injected at the eight-cell stage into the dorsal region of two dorsal–vegetal blastomeres fated to be heart and liver anlage. Electroporation of mRNA was performed essentially as described[21]. Injection of mRNA (5 ng in 5 nl of solution) into the vicinity of heart anlage and application of electric pulses were performed at stage 28. Whole-mount *in situ* hybridization analysis of murine IGFBP-4 was performed as described[30].


22. He, X. *et al.* A member of the Frizzled protein family mediating axis induction by Wnt-5A. *Science* **275**, 1652–1654 (1997).
23. Tamai, K. *et al.* LDL-receptor-related proteins in Wnt signal transduction. *Nature* **407**, 530–535 (2000).
24. Mao, B. *et al.* LDL-receptor-related protein 6 is a receptor for Dickkopf proteins. *Nature* **411**, 321–325 (2001).
25. Christian, J. L. & Moon, R. T. Interactions between Xwnt-8 and Spemann organizer signaling pathways generate dorsoventral pattern in the embryonic mesoderm of *Xenopus*. *Genes Dev.* **7**, 13–28 (1993).
26. Yost, C. *et al.* The axis-inducing activity, stability, and subcellular distribution of β-catenin is regulated in *Xenopus* embryos by glycogen synthase kinase 3. *Genes Dev.* **10**, 1443–1454 (1996).
27. Kolossov, E. *et al.* Identification and characterization of embryonic stem cell-derived pacemaker and atrial cardiomyocytes. *FASEB J.* **19**, 577–579 (2005).
28. Korchynskyi, O. & ten Dijke, P. Identification and functional characterization of distinct critically important bone morphogenetic protein-specific response elements in the Id1 promoter. *J. Biol. Chem.* **277**, 4883–4891 (2002).
29. Kishida, M. *et al.* Synergistic activation of the Wnt signaling pathway by Dvl and casein kinase Iε. *J. Biol. Chem.* **276**, 33147–33155 (2001).
30. Hosoda, T. *et al.* A novel myocyte-specific gene Midori promotes the differentiation of P19CL6 cells into cardiomyocytes. *J. Biol. Chem.* **276**, 35978–35989 (2001).

# Gremlin Enhances the Determined Path to Cardiomyogenesis

**Daisuke Kami[1,3], Ichiro Shiojima[4], Hatsune Makino[1], Kenji Matsumoto[2], Yoriko Takahashi[1], Ryuga Ishii[1], Atsuhiko T. Naito[4], Masashi Toyoda[1], Hirohisa Saito[2], Masatoshi Watanabe[3], Issei Komuro[4], Akihiro Umezawa[1]***

1 Department of Reproductive Biology, National Institute for Child Health and Development, Tokyo, Japan, 2 Department of Allergy and Immunology, National Institute for Child Health and Development, Tokyo, Japan, 3 Laboratory for Medical Engineering, Division of Materials Science and Chemical Engineering, Graduate School of Engineering, Yokohama National University, Yokohama, Japan, 4 Department of Cardiovascular Science and Medicine, Chiba University Graduate School of Medicine, Chiba, Japan

## Abstract

***Background:*** The critical event in heart formation is commitment of mesodermal cells to a cardiomyogenic fate, and cardiac fate determination is regulated by a series of cytokines. Bone morphogenetic proteins (BMPs) and fibroblast growth factors have been shown to be involved in this process, however additional factors needs to be identified for the fate determination, especially at the early stage of cardiomyogenic development.

***Methodology/Principal Findings:*** Global gene expression analysis using a series of human cells with a cardiomyogenic potential suggested *Gremlin* (*Grem1*) is a candidate gene responsible for *in vitro* cardiomyogenic differentiation. Grem1, a known BMP antagonist, enhanced DMSO-induced cardiomyogenesis of P19CL6 embryonal carcinoma cells (CL6 cells) 10–35 fold in an area of beating differentiated cardiomyocytes. The Grem1 action was most effective at the early differentiation stage when CL6 cells were destined to cardiomyogenesis, and was mediated through inhibition of BMP2. Furthermore, BMP2 inhibited Wnt/β-catenin signaling that promoted CL6 cardiomyogenesis.

***Conclusions/Significance:*** Grem1 enhances the determined path to cardiomyogenesis in a stage-specific manner, and inhibition of the BMP signaling pathway is involved in initial determination of Grem1-promoted cardiomyogenesis. Our results shed new light on renewal of the cardiovascular system using Grem1 in human.

**Citation:** Kami D, Shiojima I, Makino H, Matsumoto K, Takahashi Y, et al. (2008) Gremlin Enhances the Determined Path to Cardiomyogenesis. PLoS ONE 3(6): e2407. doi:10.1371/journal.pone.0002407

**Editor:** Hernan Lopez-Schier, Centre de Regulacio Genomica, Spain

**Received** January 15, 2008; **Accepted** May 5, 2008; **Published** June 11, 2008



**Funding:** This study was supported by a grant from the Ministry of Education, Culture, Sports, Science and Technology (MEXT) of Japan and Health and Labor Sciences Research Grants; by a Research grant on Health Science Focusing on Drug Innovation from the Japan Health Science Foundation; by the Program for Promotion of Fundamental Studies in Health Science of the Pharmaceuticals and Medical Devices Agency; by a grant from the Terumo Life Science Foundation; by a Research Grant for Cardiovascular Disease from the Ministry of Health, Labor and Welfare (MHLW); and by a Grant for Child Health and Development from the MHLW.

**Competing Interests:** The authors have declared that no competing interests exist.

* E-mail: umezawa@1985.jukuin.keio.ac.jp

## Introduction

The critical event in heart formation is commitment of mesodermal cells to a cardiomyogenic fate and their migration into anterolateral regions of the embryo during late gastrulation. In this process, morphogenic movements and cardiac fate determination are regulated by cytokines such as bone morphogenetic proteins (BMPs) [1–3], and fibroblast growth factors (FGFs) [4–7]. These secreted proteins from neighboring endoderm, ectoderm, and the mesoderm itself, play important roles in induction of cardiac transcription factors [8] and differentiation of cardiomyocytes in amphibians [9] and avians [4]. Cardiomyogenic signals, such as BMPs and FGFs, indeed activate expression of cardiac specific transcriptional factors (Csx/Nkx2.5, Gata4, Mef2c), and these transcriptional factors activate expression of circulating hormones (atrial natriuretic peptide (ANP), brain natriuretic peptide (BNP)), and cardiac specific proteins (myosin heavy chain (MyHC), myosin light chain (MyLC)). Wnt family proteins, cysteine-rich, and secreted glycoproteins, have also been implicated in embryonic development [10,11], and cardiomyogenesis [12,13]. In *Drosophila*, '*wingless*', a homologue of vertebrate Wnt is involved in expression of '*tinman*', a *Drosophila* homologue of Csx/Nkx2.5, through '*armadillo*', a *Drosophila* ortholog of β-catenin, and drives heart development [14]. In vertebrates, however, Wnt1/3a, which activates the canonical Wnt/β-catenin signaling pathway leading to stabilization of β-catenin as a downstream molecule through inactivation of glycogen synthase kinase-3β, inhibits cardiomyocytic differentiation from cardiac mesoderm [15–18]. Wnt11 promotes cardiac differentiation via the non-canonical pathway in *Xenopus* [12] and murine embryonic cell lines [19]. The secretion of Wnt inhibitors such as 'Cerberus', 'Dickkopf' and 'Crescent' by the anterior endoderm prevents Wnt3a secreted by the neural tube from inhibiting heart formation [15–17].

In this study, we performed GeneChip analysis to identify multiple extracellular determinants, such as cytokines, cell

membrane-bound molecules and matrix responsible for cardiomyogenic differentiation, and evaluated the statistical significance of differential gene expression by NIA array analysis (http://lgsun.grc.nia.nih.gov/ANOVA/) [20], a web-based tool for microarray data analysis. We found that Grem1 enhances the determined path to cardiomyogenesis in a stage-specific manner, and that inhibition of the BMP signaling pathway is, at least in part, involved in initial determination of Grem1-promoted cardiomyogenesis.

## Results

### GeneChip and statistical analysis

To identify cytokines and transcription factors responsible for cardiomyogenic differentiation, 69 human cells were analyzed, depending on gene expression levels, by GeneSpringGX software, and clustered into 30 groups (Fig. 1A, Table 1). Among the 30 groups, 21 groups included cells with a cardiomyogenic potential (Fig. 1B: red numbers). To identify genes specific for these groups, hierarchical clustering was employed, using the average distance method. Genes with the lowest average expression E(G1) within the cluster that can differentiate into cardiomyocytes and genes with the highest average expression E(G2) outside the cluster were identified, as previously described [20–22]. Genes which have E(G1)>E(G2) were estimated, using the False Discovery Rate (FDR<0.05). Grem1 was nominated as a cluster-specific cardiomyocyte-promoting gene in cells that could differentiate into cardiomyocytes following NIA array analysis (Fig. 1B). The gene expression profile reported in this paper has been deposited in the Gene Expression Omnibus (GEO) database (http://www.ncbi.nlm.nih.gov/geo: accession no. GSE8481, GSM41342-GSM41344, and GSM201137- GSM201145).

### Cardiomyogenic differentiation of CL6 cells with Grem1 and DMSO

To investigate cardiomyogenic activity of Grem1, P19CL6 embryonal carcinoma cells (CL6 cells) were used for assessment of *in vitro* cardiomyogenic differentiation, since CL6 cells are reproducibly and stably induced into beating cardiomyocytes by DMSO (Fig. 2Aa) [23]. CL6 cells did not differentiate following exposure to Grem1 alone at concentrations of 63 or 125 ng/ml for 14 days (Fig. 2B). However, Grem1 dramatically promotes DMSO-induced cardiomyogenic differentiation at a concentration of 63 and 125 ng/ml; Grem1 (125 ng/ml) especially increased DMSO-induced cardiomyogenic differentiation of CL6 cells as assessed by beating area (Fig. 2Ab and B) (Movie S1 and S2, http://1954.jukuin.keio.ac.jp/umezawa/kami/index.html).

### RT-PCR of differentiated or undifferentiated CL6 cells

To investigate gene expression as well as morphological analysis, i.e. beating, during cardiomyogenic differentiation, RT-PCR analysis was performed to detect expression of cardiomyocyte-specific/associate transcription factors, and structural genes (Fig. 2C). Genes encoding *Csx/Nkx2.5*, *Gata4*, *Hand2*, *Mef2c*, *ANP*, *BNP*, *MyLC-2a*, *MyLC-2v*, and *β-MyHC* were up-regulated during cardiomyogenic differentiation of CL6 cells treated with Grem1 and DMSO (Fig. 2C: lanes 6, 7 versus lane 3). Triplicate independent experiments confirmed the concentration-dependent Grem1 action on cardiomyogenic differentiation. The cardiomyocyte-specific genes (*Csx/Nkx2.5*, *Gata4*, *MyLC-2a*, *MyLC-2v*) expression level of CL6 cells treated with DMSO and Grem1 (63 and 125 ng/ml) were also the same as or higher than that of DMSO-induced CL6 cells by semi-quantitative RT-PCR (Figure S1).

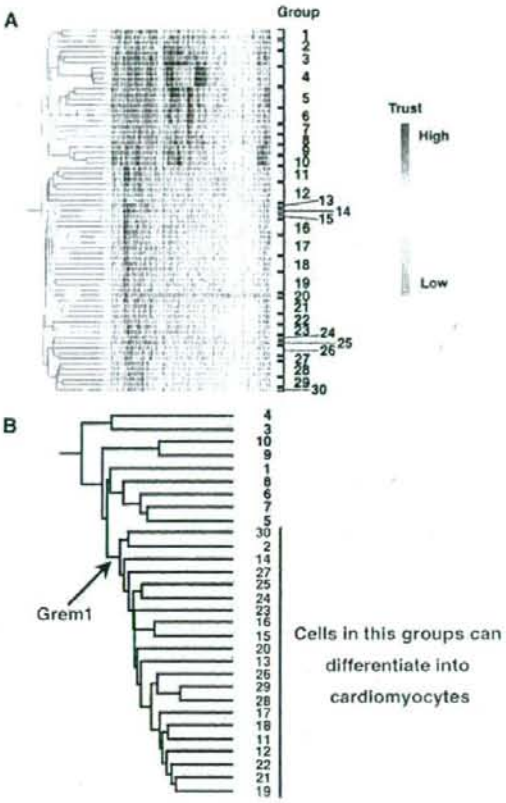


**Figure 1. Hierarchical clustering analysis on cultured human cells. (A)** Hierarchical clustering analyzed by GeneSpring. Based on gene expression pattern, 69 human cells were clustered into 30 sub-groups. The raw data from the GeneChip analysis are available at the GEO database with accession number GSE8481, GSM41342- GSM41344, and GSM201137- GSM201145. **(B)** Hierarchical clustering analysis was performed by NIA array (http://lgsun.grc.nia.nih.gov/ANOVA/), using averaged values of 30 sub-groups. Among the 30 groups, 21 groups included cells with a cardiomyogenic potential. To identify genes specific for these groups, hierarchical clustering was employed. *Grem1* was nominated as a cluster-specific cardiomyocyte-promoting gene in cells that could differentiate into cardiomyocytes.
doi:10.1371/journal.pone.0002407.g001

### Immunocytochemistry of differentiated or undifferentiated CL6 cells

To examine CL6 cells for expression of cardiomyocytic protein, immunocytochemical analysis was performed. CL6 treated with Grem1 (125 ng/ml) and DMSO exhibited clear striation with immunostain using anti-cTnT or anti-α-actinin (Fig. 2Da and b). The MF20- and cTnT-positive cells after exposure to Grem1 and DMSO formed clusters (Fig. 2Ea), compared with the cells after exposure to DMSO alone (Fig. 2Eb). CL6 cells treated with Grem1 alone were negative for MF20 and cTnT, but became positive for both markers following exposure to Grem1 (63 and 125 ng/ml) and DMSO (Fig. 2F). The beating area (Fig. 2B) showed a tendency similar to the MF20- and cTnT-positive area (Fig. 2F), thus there were positive correlations between them.

**Table 1.** 69 human cells clustered into 30 groups

| Group | | Title | Description | GSM |
|---|---|---|---|---|
| 1 | Normal epithelial cell,primary | NHEK-Neo1 | Normal epidermal keratinocyte, neonate, primary | GSM210361 |
| | | NHBE-1 | Normal bronchial epithelial cell, primary | GSM210362 |
| 2 | Pulmonary epithelial cell line | A549 | Pulmonary epithelial cell line | GSM210363 |
| | | BEAS-2B control (6hr) | Bronchial epithelial cell line | GSM210364 |
| 3 | Lymphocyte | RPMI8226control (6hr) | B cell line | GSM210365 |
| | | Raji-1 | B cell line | GSM210366 |
| | | NK92 | NK cell line | GSM210367 |
| 4 | Myelomonocytic leukemia | U937c | U937 control | GSM210368 |
| | | U937h | U937+HRF | GSM210369 |
| | | U937ha | U937+HRF+antibody | GSM210370 |
| | | U937a | U937+antibody | GSM210371 |
| 5 | Embryonal carcinoma, cancer | NCR-G3 | Embryonal carcinoma, NCR-G3, non-adherent | GSM201141 |
| | | NCR-G2NAd | Embryonal carcinoma, NCR-G2, non-adherent | GSM210373 |
| | | NCR-G4Ad | Embryonal carcinoma, NCR-G4, adherent | GSM201142 |
| | | NCR-G3Ad | Embryonal carcinoma, NCR-G3, adherent | GSM210375 |
| 6 | ES cell | H1_P43 | Undifferentiated hES | GSM41342 |
| | | H1-P46 | Undifferentiated hES | GSM41343 |
| | | H1-P41 | Undifferentiated hES | GSM41344 |
| 7 | Embryonal carcinoma, cancer | NCR-G2Ad | Embryonal carcinoma, NCR-G2, adherent | GSM201140 |
| | | NCR-G1 | Embryonal carcinoma, NCR-G3, non-adherent | GSM201139 |
| 8 | Ewing, cancer | NCR-EW2 | Ewing, cancer | GSM210378 |
| | | NCR-EW3 | Ewing, ETV4, cancer | GSM210379 |
| 9 | Ewing, cancer | GST6 | Ewing, POU5F1, cancer | GSM201137 |
| | | GST6-extra | Ewing, POU5F1, cancer | GSM210381 |
| 10 | Ewing, cancer | GST6-5az | Ewing, POU5F1, 5azaC, cancer | GSM201138 |
| | | GST6-5az-extra | Ewing, POU5F1, 5azaC, cancer | GSM210383 |
| 11 | Bone marrow cell, primary | H4-1 | Bone marrow cell, primary | GSM201143 |
| | | UBT5 | Bmi-1, hTERT, bone marrow cell | GSM210385 |
| | | UBET7 | Bmi-1, E6, hTERT, bone marrow cell | GSM210386 |
| 12 | Ligament-derived cells | #10 | Ligament, primary | GSM210387 |
| | Marrow stromal cells | H10-2Vec | Vector, bone marrow cell | GSM210388 |
| | | H10-2TERT | hTERT, bone marrow cell | GSM210389 |
| | | H10-2Bmi1 | Bmi-1, bone marrow cell | GSM210390 |
| 13 | Placenta, primary | PL90 | Placenta, primary | GSM210391 |
| 14 | De-differentiated chondrocyte | TdHC1 | E6, E7, hTERT, de-differentiated chondrocyte | GSM210392 |
| 15 | Neural differentiated marrow stromal cell | UET13 Neural differentiation | E7, hTERT, neural differentiation, bone marrow cell | GSM210393 |
| 16 | Neural differentiated marrow stromal cell | UET13 Neural differentiation1 | E7, hTERT, neural differentiation, bone marrow cell | GSM210394 |
| | | UET13 Neural differentiation4 | E7, hTERT, neural differentiation, bone marrow cell | GSM210395 |
| | | UET13 Neural differentiation5 | E7, hTERT, neural differentiation, bone marrow cell | GSM210396 |
| 17 | Cord blood-derived cells | UET13 | E7, hTERT, bone marrow cell | GSM210397 |
| | | UCB408 | Cord blood, primary | GSM210398 |
| | | UCB408E6E7-31 | E6, E7, umbilical cord blood | GSM210399 |
| | Adipocyte cell, primary | HAdPC1(5/21) | HAdpc1E6E7TERT28 | GSM210400 |
| 18 | Marrow mesenchymal cell, primary | UEET12 | E6, E7, hTERT, bone marrow cell | GSM210401 |
| | | UEE16 | E6, E7, bone marrow cell | GSM210402 |
| | | EPC hTERT+1 | E6, E7, hTERT, endometrial cell | GSM201144 |
| 19 | Cord blood, primary | UCB302 | Cord blood, primary | GSM210382 |
| | | UCB302-D7 | Cord blood, primary | GSM210405 |
| | | UCB302TERT | hTERT, cord blood | GSM210406 |
| | | UET9 | E7, hTERT, bone marrow cell | GSM210407 |

**Table 1.** cont.

| Group | | Title | Description | GSM |
|---|---|---|---|---|
| 20 | Cord blood, primary | UCB408E7-32 | E7, hTERT, cord blood | GSM210408 |
| 21 | Fetal fibroblast, primary | HFDPC cont. | Normal follicular dermal papillar cell, primary | GSM210409 |
| | | PL112 | Placenta, primary | GSM210410 |
| | | HF7-3 | Fetal fibroblast, primary | GSM210411 |
| 22 | Bone marrow cell, primary | 3F0664 | Bone marrow cell (commercial item), primary | GSM201145 |
| | | BM-MSC | Bone marrow-derived mesenchymal stem cells | GSM38627 |
| 23 | ES cell-derived mesenchymal cell | H1 clone 2 | ES cell-derived mesenchymal precursor | GSM38628 |
| | | H9 clone 1 | ES cell-derived mesenchymal precursor | GSM38629 |
| 24 | Endometrial cell | EPC100 | E6, E7, hTERT, endometrial cell | GSM210413 |
| 25 | Bone marrow cell, primary | Yub10F | Bone marrow cell, primary | GSM210414 |
| 26 | Endometrial cell | EPC hTERT+2 | E6, E7, hTERT, endometrial cell | GSM210415 |
| | | EPC Control | E6, E7, hTERT, endometrial cell | GSM210416 |
| 27 | Endometrial cell | EPC214 | E6, E7, hTERT, endometrial cell | GSM210417 |
| 28 | Menstruation blood-derived mesenchymal cell, primary | #E4 | Menstruation blood, primary | GSM210418 |
| | | #E4HRF | Menstruation blood, HRF treatment, primary | GSM210419 |
| | | #E5HRF | Menstruation blood, HRF treatment, primary | GSM210420 |
| 29 | Menstruation blood-derived mesenchymal cell, primary | #E6 | Menstruation blood, primary | GSM210421 |
| | | #E6HRF | Menstruation blood, HRF treatment, primary | GSM210422 |
| 30 | Menstruation blood-derived mesenchymal cell, primary | #E5 | Menstruation blood, primary | GSM210423 |

doi:10.1371/journal.pone.0002407.t001

## Grem1 and DMSO were most effective at the early stage (days 1–3) of CL6 differentiation

To determine if Grem1 (125 ng/ml) functions during the early or the late stage of differentiation, CL6 cells were treated with Grem1 for different time periods (Fig. 3A). Grem1 and DMSO were most effective on CL6 differentiation at 1–3 days (Fig. 3B, C) as assessed by percentages of MF20-positive area and beating area. Since Grem1 inhibits BMPs through direct binding [24], we hypothesized that BMP signaling is inhibitory to CL6 cardiomyogenesis during days 1–3. To confirm this hypothesis, RT-PCR analysis was performed to determine expression of the early mesodermal marker (*BrachyuryT* and *Tbx6*), cardiomyocyte-specific transcription factors (*Csx/Nkx2.5*), structural genes (*β-MyHC*), and *Gapdh* (Fig. 4A). DMSO induced the *BrachyuryT* and *Tbx6* genes, and their expressions peaked at 3 days and then decreased; BMP2 down-regulated expression of these genes at 3–7 days. The *Csx/Nkx2.5* and *β-MyHC* genes started to be expressed at days 3 and 5, respectively, and their expression increased up to 14 days, at which time the timeframe analysis was terminated. BMP2 clearly inhibited expression of the *Csx/Nkx2.5* and *β-MyHC* genes (Fig. 4A, lanes 1–7 versus lanes 8–14).

To examine cardiomyogenic differentiation, immunocytochemical analysis was performed on CL6 cells treated with the inducers. CL6 cells treated with DMSO and BMP2 for the first 3 days were negative for sarcomeric myosin (MF20) at 14 days, but became positive for sarcomeric myosin, following exposure to DMSO alone during days 1–3 (Fig. 4B). To determine if DMSO induces BMP production in CL6 cells, expression levels of *Bmp2* and *Bmp4* were determined by quantitative real-time RT-PCR analysis (Fig. 4C). DMSO clearly induced the *Bmp2* and *Bmp4* genes, and DMSO-induction was inhibited by BMP2 protein. The expression level of *Bmp2* was highest during days 7–10 (Fig. 4C: *Bmp2*) in DMSO-induced CL6 cells, and that of *Bmp4* was highest during days 5–7 (Fig. 4C: *Bmp4*).

To investigate BMP signaling on cardiomyogenic differentiation, we used the *Id1* promoter-Lux plasmid that includes the luciferase gene driven by the *Id1* promoter, known as a BMP target promoter (Fig. 4D). DMSO increased BMP signaling activity that peaked at 5 days (Fig. 4D, open square). BMP2 protein increased BMP signaling activity at 3 days (Fig. 4D, closed square), but lost BMP signaling activity at 5 days and later, implying that this loss of BMP signaling leads to lack of cardiomyogenic induction.

Since Wnt/β-catenin signaling is involved in CL6 cardiomyogenesis [23,25], we hypothesized that the BMP effect on CL6 cardiomyogenesis is mediated through Wnt/β-catenin signaling. Expression of Wnt3a, an activator of canonical Wnt signaling, was indeed detected in CL6 cells exposed to DMSO, and BMP2 significantly down-regulated *Wnt3a* expression at day 3 (Fig. 4E). By using the TOPflash plasmid [23] which includes the luciferase gene driven by two sets of three copies of the TCF recognition site, Wnt/β-catenin signaling was assessed to investigate the effect of BMP2. Wnt/β-catenin signaling activity increased at 48 h after treatment with DMSO. Activity was increased by DMSO treatment but decreased by BMP2 (Fig. 4F). Time course analysis revealed that Wnt/β-catenin activity peaked at 5 days after DMSO treatment, and decreased thereafter (Fig. 4G). BMP2 inhibited DMSO-induced Wnt/β-catenin activity throughout the experimental period (up to 14 days). These results imply that BMP signaling inhibits CL6 cardiomyogenesis at the early stage through inhibition of Wnt/β-catenin signaling.

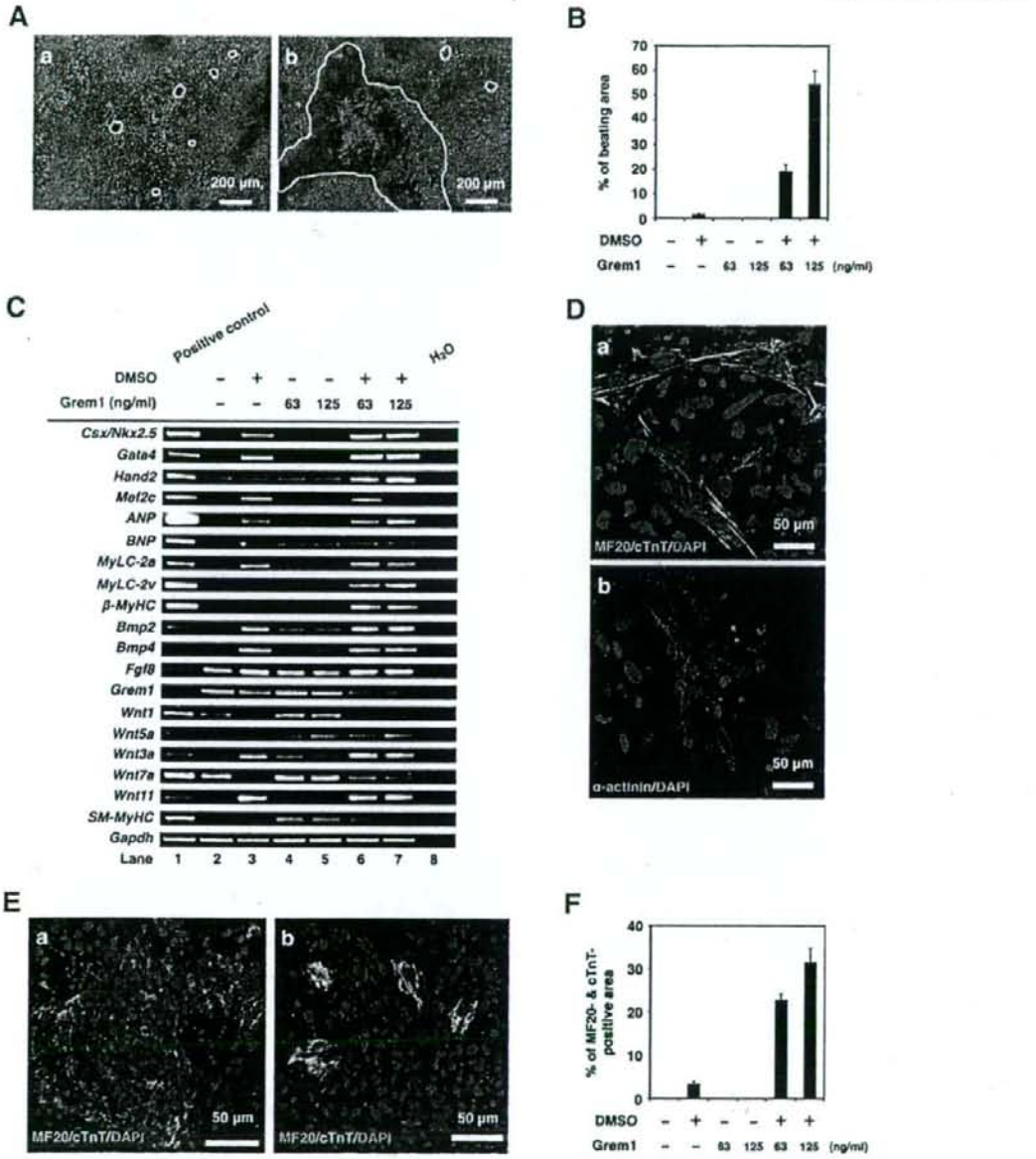


**Figure 2. Grem1 enhanced cardiomyogenic differentiation in DMSO-induced CL6 cells. (A)** Phase contrast micrograph of CL6 cells with exposure to DMSO alone (a), Grem1 (125 ng/ml) and DMSO (b) for 14 days. The medium, including Grem1 and DMSO, was changed every day. CL6 cells exhibited apparent spontaneous beating between days 9–11. Beating CL6 cell colonies are outlined by white lines. **(B)** Percentage of beating area in differentiated CL6 cells. CL6 cell treated with Grem1 (125 ng/ml) and DMSO exhibited the strongest contraction. **(C)** RT-PCR analysis of the genes encoding cardiac-specific transcriptional factors (*Csx/Nkx2.5, Gata4, Mef2c, Hand2*), circulating hormone (*ANP, BNP*), cardiac-specific proteins (*MyLC-2a, MyLC-2v, β-MyHC*), cytokines (*Bmp2, Bmp4, Fgf8, Grem1, Wnt1, Wnt3a, Wnt5a, Wnt7a, Wnt11*), *SM-MyHC*, and *Gapdh* (From top to bottom). Mouse total heart RNA for the *Csx/Nkx2.5, Gata4, Mef2c, Hand2, ANP, BNP, MyLC-2a, MyLC-2v, β-MyHC, Bmp2, Bmp4, Grem1, Wnt11, SM-MyHC*, and *Gapdh* genes, mouse embryonic stem cell RNA for the *Fgf8* gene, and mouse total skeletal muscle RNA for the *Wnt1, Wnt3a, Wnt5a*, and *Wnt7a* genes were used for positive controls. $H_2O$ (without RNA) served as a negative control. **(D)** Immunocytochemistry of CL6 cells 14 days after exposure to Grem1 (125 ng/ml) and DMSO with MF20 and cTnT (a), and α-actinin (b). Cell nuclei are stained with DAPI. Clear striations are evident. **(E)** Immunocytochemistry of CL6 cells 14 days after exposure to Grem1 and DMSO with cardiac troponin T (cTnT) and sarcomeric myosin (MF20). CL6 cells treated with Grem1 (125 ng/ml) and DMSO (a), and DMSO alone (b) stained positive for cTnT and MF20. Untreated CL6 cells, i.e. not exposed to Grem1(125 ng/ml) or DMSO, stained negative for cTnT and MF20. Cell nuclei were stained with DAPI. **(F)** Percentage of MF20- and cTnT-double positive area.
doi:10.1371/journal.pone.0002407.g002

**A**

| | Day | 0 | 1 | 2 | 3 | 4 | 5 | 6 | 7 | 8 | 9 | 10 | 11 | 12 | 13 | 14 |
|---|---|---|---|---|---|---|---|---|---|---|---|---|---|---|---|---|
| DMSO | – | – | – | – | – | – | – | – | – | – | – | – | – | – | – | – |
| Grem1 | – | – | – | – | – | – | – | – | – | – | – | – | – | – | – | – |
| DMSO | 1-14 | – | + | + | + | + | + | + | + | + | + | + | + | + | + | + |
| Grem1 | – | – | – | – | – | – | – | – | – | – | – | – | – | – | – | – |
| DMSO | 1-14 | – | + | + | + | + | + | + | + | + | + | + | + | + | + | + |
| Grem1 | 1-3 | – | + | + | + | – | – | – | – | – | – | – | – | – | – | – |
| DMSO | 1-14 | – | + | + | + | + | + | + | + | + | + | + | + | + | + | + |
| Grem1 | 4-7 | – | – | – | – | + | + | + | + | – | – | – | – | – | – | – |
| DMSO | 1-14 | – | + | + | + | + | + | + | + | + | + | + | + | + | + | + |
| Grem1 | 8-14 | – | – | – | – | – | – | – | – | + | + | + | + | + | + | + |
| DMSO | 1-3 | | + | + | + | – | – | – | – | – | – | – | – | – | – | – |
| Grem1 | – | – | – | – | – | – | – | – | – | – | – | – | – | – | – | – |
| DMSO | 1-14 | – | + | + | + | + | + | + | + | + | + | + | + | + | + | + |
| Grem1 | 1-14 | – | + | + | + | + | + | + | + | + | + | + | + | + | + | + |
| DMSO | 1-14 | – | + | + | + | + | + | + | + | + | + | + | + | + | + | + |
| Grem1 | 1-3 | – | + | + | + | – | – | – | – | – | – | – | – | – | – | – |
| DMSO | 1-3 | – | + | + | + | – | – | – | – | – | – | – | – | – | – | – |
| Grem1 | 1-3 | – | + | + | + | – | – | – | – | – | – | – | – | – | – | – |

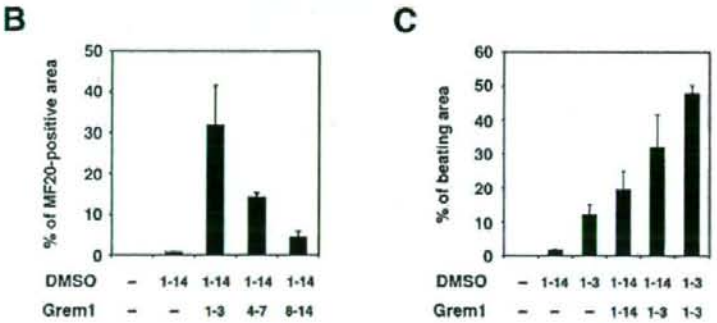


**Figure 3. Percentage of myogenic differentiation by period of treatment with Grem1 in CL6 cells. (A)** Protocol for treatment of Grem1 and DMSO. CL6 cells were passaged at $1.8\times10^5$ cells in 6-well plate on Day 0. CL6 cells were exposed to Grem1 (125 ng/ml) and/or DMSO on the indicated day. Day when the cells were exposed to the inducers is shown by "+" (in gray cells for clarity). The medium including Grem1 and DMSO was changed every day. On day 14, the cells were immunocytochemically stained with MF20 antibody. **(B)** Myogenic differentiation of CL6 cells was estimated by sarcomeric myosin (MF20)-positive area. CL6 cells were treated with Grem1 (125 ng/ml) and DMSO for the indicated days. **(C)** Myogenic differentiation of CL6 cells was estimated by beating area. CL6 cells treated with DMSO and Grem1 (125 ng/ml) were incubated at indicated days.
doi:10.1371/journal.pone.0002407.g003

## Discussion

Our bioinformatics study using the results from the global gene expression analysis of human cells (GSM412342-41344 and GSM201137-201145 at http://www.ncbi.nlm.nih.gov/geo) nominated Grem1 as a candidate gene that may participate in cardiomyogenesis. By using CL6 embryonic cells as a model of cardiomyogenesis, we obtained two major findings: the first is that Grem1 enhanced cardiomyogenic differentiation of DMSO-induced CL6 cells at the early stage; the second is that Wnt/β-catenin and BMP signaling activity had developmental stage-specific effects on cardiomyogenesis (Fig. 5). Wnt/β-catenin activity at the early stage enhanced embryonic cell differentiation into cardiomyocytes, while suppressing this activity by BMP2 or BMP4 proteins as reported in the avian embryo [26]. In contrast, BMP signaling activity in the late stage enhanced cardiomyocytic differentiation. Grem1 regulated the stage-specific Wnt/β-catenin and BMP signaling activity on cardiomyogenesis.

Many studies have indicated that Grem1 is involved in cell differentiation and development, such as osteogenesis [27], lung morphogenesis [28], myogenesis [29], and limb formation [30], through inhibition of BMP2 and BMP4. Grem1-null mice show intact heart development, despite impairment of lung and kidney [31], and therefore Grem1 is considered not to be involved in cardiogenesis, or supplementary factors such as Noggin [32], with a similar function, may compensate Grem1 during development. Grem1 had an enhancing or promoting activity in *in vitro* cardiomyogenesis, as is the case with platelet-derived growth factor as a promoter of cell growth [33]. In this study, Grem1 was involved in cardiomyocyte differentiation. However Grem1 alone could not induce cardiomyocytic differentiation of CL6 cells in the absence of DMSO (Fig. 2C and F), suggesting that Grem1 is solely

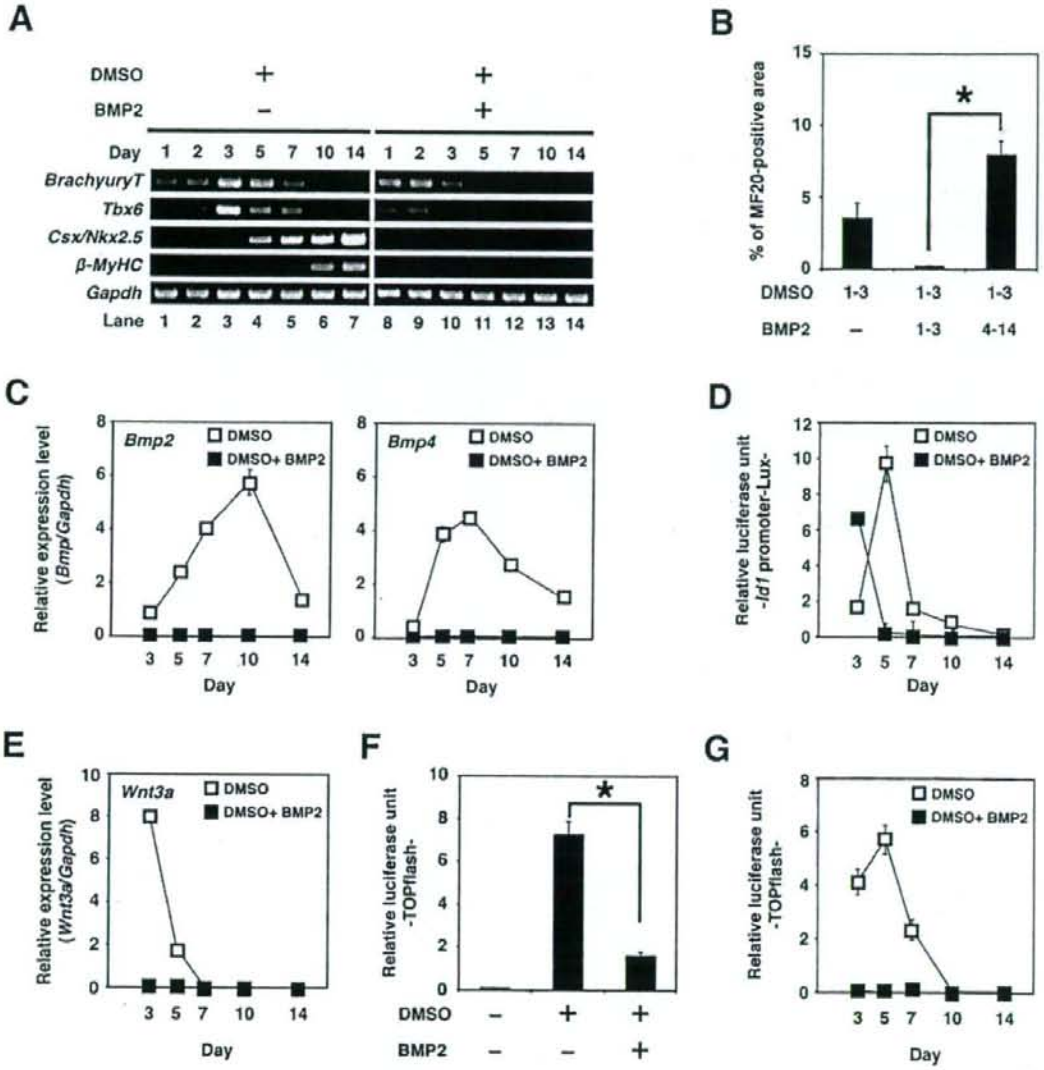


**Figure 4. Cardiomyogenic differentiation in CL6 cells (days 1–3) is inhibited by BMP2.** **(A)** RT-PCR analysis of the gene encoding *BrachyuryT*, *Tbx6*, cardiac-specific transcriptional factor (*Csx/Nkx2.5*), cardiac-specific protein (*β-MyHC*), and *Gapdh* (From top to bottom) of CL6 cells treated with DMSO alone, or DMSO and BMP2 (100 ng/ml) for the first 3 days (days 1–3). The medium, including BMP2 and DMSO, was changed every day. **(B)** Percentage of MF20-positive area. Immunocytochemistry was carried out on CL6 cells 14 days after cells had been exposed to DMSO and BMP2 (100 ng/ml) for the first 3 days (days 1–3). The asterisk indicates a significant statistical difference ($P<0.05$). **(C)** Quantitative real-time RT-PCR analysis of the gene encoding *Bmp2* (left), and *Bmp4* (right) in CL6 cells treated with DMSO alone (open square), or DMSO and BMP2 (100 ng/ml) (closed square) for the first 3 days (days 1–3). **(D)** BMP signaling activity of CL6 cells treated with DMSO alone (open square), or DMSO and BMP2 (100 ng/ml) (closed square) for the first 3 days (days 1–3) were determined by luciferase activity analysis using *Id1* promoter-Lux (a firefly luciferase reporter plasmid driven by the Id1 binding sites), pRL-CMV as co-transfected control, and Dual luciferase reporter assay system. Relative luciferase unit of the CL6 cells untreated with inducers at day 3 is regarded as 0.1 (data not shown). **(E)** Quantitative real-time RT-PCR analysis of the gene encoding *Wnt3a* in CL6 cells treated with DMSO alone (open square), or DMSO and BMP2 (100 ng/ml) (closed square) for the first 3 days (days 1–3). **(F)** Wnt/β-catenin signaling activity of CL6 cells 48 h after exposure to DMSO, or DMSO and BMP2 (100 ng/ml) was determined by luciferase activity analysis using TOPflash (a firefly luciferase reporter plasmid driven by two sets of three copies of the TCF binding site and herpes simple virus thymidine kinase minimal promoter), pRL-CMV as co-transfected control, and Dual luciferase reporter assay system. Relative luciferase unit of the CL6 cells untreated with inducers is regarded as 0.1. The asterisk indicates a significant statistical difference ($P<0.05$). **(G)** Timeframe of Wnt/β-catenin signaling activity in CL6 cells treated with DMSO alone (open square), or DMSO and BMP2 (100 ng/ml) (closed square) for the first 3 days (days 1–3). Relative luciferase unit of the CL6 cells untreated with inducers at day 3 is regarded as 0.1 (data not shown).
doi:10.1371/journal.pone.0002407.g004

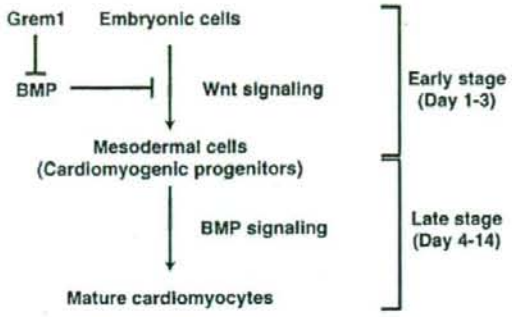


**Figure 5. Grem1-accelerated CL6 cardiomyogenesis through regulation of BMP- and Wnt/β-catenin-signaling pathways.** CL6 embryonic cells start to differentiate into mesodermal cells through Wnt/β-catenin signaling pathway at the early stage (days 1–3), and mesodermal CL6 cells differentiate into mature cardiomyocytes by BMP pathway at the late stage (days 4–14). Grem1 accelerates DMSO-induced cardiomyogenesis through inhibition of the BMP-signaling pathway.
doi:10.1371/journal.pone.0002407.g005

a promoter of cardiomyogenic differentiation. One of the possible mechanisms for Grem1-enhanced cardiomyogenesis at the early stage is inhibition of the BMP signaling pathway [3]. Alternatively, Grem1-enhanced cardiomyogenesis may be mediated through proliferation of cardiac progenitor cells, as is the case of myogenic progenitor proliferation by Grem1 [34], and this possibility is supported by an increased number of sarcomeric myosin-positive CL6 cardiomyocytes (Fig. 2E and F).

The stage specificity of the Grem1 effect is possibly correlated with the biphasic and antagonistic effect of Wnt/β-catenin signaling on cardiomyogenesis, depending on the stage of development *in vitro* [25] and *in vivo* [35]. CL6 cells differentiated into cardiomyocytes via mesodermal induction by the Wnt/β-catenin signaling pathway at the early stage, and CL6 mesodermal cells differentiated into cardiomyocytes induced by BMP2 at the late stage. It is conceivable that embryonic cells, such as CL6 cells and ES cells, differentiate into cardiomyocytes by inhibiting BMP signaling via putative "mesodermal cells" or "cardiomyogenic progenitors", or differentiation stages corresponding to these cells (Fig. 5, Figure S2). The early stage process from embryonic cells to mesodermal cells was mediated via Wnt/β-catenin signaling (Fig. 4F, G), and was assessed by expression of *BrachyuryT* and *Tbx6* genes (Fig. 4A), which are target genes for Wnt/β-catenin signaling [36]. BMP signaling antagonizes the cell fate-inducing activity of Wnt/β-catenin [37]. When embryonic cells or cardiomyogenic progenitors are induced to become mature cardiomyocytes by cytokines and growth factors, we must be careful with respect to the stage of cell differentiation because of the biphasic differential action of the factors which are dependent upon the differentiation stage.

In conclusion, we have demonstrated that Grem1 enhances the commitment or determined path to cardiogenic differentiation of CL6 teratocarcinoma cells. Apart from a role in development, Grem1 may serve a clinical use in cardiology, like granulocyte colony-stimulating factor that accelerates production of granulocytes in both peripheral blood and bone marrow. Nomination of *Grem1* as a cardiomyogenic factor is based on hierarchical clustering analysis using global gene expression data of human cells. This bioinformatics approach may be useful for identifying morphogens/factors that can induce differentiation of other cell types/tissues/organs.

## Materials and Methods

### GeneChip analysis

GeneChip analysis was performed (Fig. 1A, Table 1) as previously described [38]. Human genome-wide gene expression was examined with the Human Genome U133A Probe array (GeneChip; Affymetrix), which contains the oligonucleotide probe set for approximately 23,000 full-length genes and expressed sequence tags, according to the manufacturer's protocol (Expression Analysis technical manual and GeneChip Small Sample Target Labeling Assay version 2 technical note [http://www.affymetrix.com/support/technical/index.affx]). Data analysis was performed by the GeneChip Operation System (Affymetrix) and GeneSpringGX software (Silicon Genetics). To normalize the staining intensity variations between chips, the average difference values for all genes on a given chip were divided by the median of all measurements on that chip. Hierarchical-clustering analysis was performed using a minimum distance value of 0.001, a separation ratio of 0.5, and the standard definition of the correlation distance.

### Cell culture and differentiation

CL6 cells were grown on 100 mm dishes (Becton Dickinson) in α-MEM (Gibco) supplemented with 10% fetal bovine serum (FBS) (JRH Bioscience, Inc.), penicillin, and streptomycin, and were maintained in a 5% $CO_2$ atmosphere at 37°C. To induce differentiation, CL6 cells were plated at a density of $1.8\times10^5$ cells in a 6-well plate (Becton Dickinson) or gelatin-coated 35 mm glass base dishes (IWAKI) with α-MEM containing Grem1 (63 or 125 ng/ml: R&D system) and/or 1% dimethyl sulfoxide (DMSO) for 14 days. Recombinant human bone morphogenetic protein-2 (BMP2) was purchased from R&D systems.

### Reverse transcriptase-PCR (RT-PCR) and quantitative real-time RT-PCR analysis

Total RNAs were extracted from differentiated and undifferentiated CL6 cells and mouse embryonic stem (ES) cells with RNeasy minikit and DNase I treatment (QIAGEN). Mouse ES cell (129 strains) RNA, mouse heart total RNA (Clontech) and mouse skeletal muscle/total RNA (UNITECH. Co., Ltd.) were used as a positive control for each primer. Total RNA (2.0 μg each) for RT-PCR was converted to cDNA with Superscript™ III RNase H– reverse transcriptase (Invitrogen), according to the manufacturer's manual. PCR conditions were optimized and linear amplification range was determined for each primer by varying annealing temperature and cycle number. PCR products were identified by positive control size. RT-PCR was performed using the primers of the genes of cardiac specific transcription factors: *Csx/Nkx2.5*, *Gata4*, *Mef2c*, *Hand2*; circulating hormone: *ANP*, *BNP*; cardiac structural proteins: *β-MyHC*, *MyLC-2a*, *MyLC-2v*; cytokines: *Bmp2*, *Bmp4*, *Fgf8*, *Grem1*, *Wnt1*, *Wnt3a*, *Wnt5a*, *Wnt7a*, *Wnt11*; smooth muscle structural protein: smooth muscle-myosin heavy chain (*SM-MyHC*); the early mesodermal marker: *BrachyuryT*, *T-box6* (*Tbx6*); and *Gapdh* as control. PCR was performed with exTaq DNA polymerase and exTaq PCR buffer (TaKaRa) or LATaq DNA polymerase and GC buffer I (TaKaRa) for 25 or 30 cycles, with each cycle consisting of 95°C for 30 s, 50°C, 55°C, 60°C or 65°C for 45 s, and 72°C for 45 s, with an additional 5 min incubation at 72°C after completion of the final cycle. PCR primers for the genes of *Csx/Nkx2.5*, *Gata4*, *Mef2c*, *Hand2*, *ANP*, *BNP*, *β-MyHC*, *MyLC-2a*, *MyLC-2v*, *Bmp2*, *Bmp4*, *Fgf8*, *Grem1*, *Wnt1*, *Wnt3a*, *Wnt5a*, *Wnt7a*, *Wnt11*, *SM-MyHC*, *BrachyuryT*, *Tbx6*, and *Gapdh* (Table S1a) were obtained from Mouse Genome

Informatics (http://www.informatics.jax.org/). The PCR products were size-fractionated by 2% agarose gel electrophoresis.

Quantitative real-time RT-PCR was performed on an ABI Prism 7700 Sequence Detection System (Applied Biosystems), using 100 ng of cDNA in 25 μl reaction volume with 10 nmol/l of each primer, and 12.5 μl SYBR Green Realtime PCR Master Mix (TOYOBO). PCR primers for the genes of *Bmp2*, *Bmp4*, *Wnt3a*, and *Gapdh* (Table S1b) were obtained from PrimerBank (http://pga.mgh.harvard.edu/primerbank/index.html). Calculations were automatically performed by ABI software (Applied BioSystems).

### Immunocytochemistry

A laser confocal microscope (LSM510, Zeiss) was used for immunocytochemical analysis. Differentiated and undifferentiated CL6 cells were fixed with 4% paraformaldehyde (Wako) for 5 min at 4°C and treated with 0.1% triton X-100 (Sigma) in PBS for 20 min at room temperature, then incubated for 20 min at room temperature in a protein-blocking solution consisting of PBS supplemented with 5% normal goat serum (DakoCytomation). These CL6 cells were then incubated overnight with primary antibody monoclonal anti-sarcomeric myosin antibody (MF20, mouse $IgG_{2b}$, isotype, 1 mg/ml, University of Iowa Hybridoma Bank) and Troponin T, and Cardiac Isoform Ab-1 clone 13-11 (cTnT, mouse $IgG_1$ isotype, 1:300, Lab Vision Corp), or the monoclonal anti-α-actinin (SARCOMERIC) CLONE EA-53 (α-actinin, mouse $IgG_1$ isotype, 1:300, Sigma) in PBS at 4°C. The cells were extensively washed in PBS and incubated at room temperature with Alexa Fluor 568-conjugated goat anti-Mouse $IgG_{2b}$, (anti-MF20) (Molecular Probe; diluted 1:300), Alexa Fluor 488-conjugated goat anti-mouse $IgG_1$ (anti-cTnT) (Molecular Probe; diluted 1:300), Alexa Fluor 546-conjugated goat anti-mouse IgG(H+L) (anti-α-actinin) (Molecular Probe; diluted 1:300), and nuclei were counterstained with 4′, 6-diamidino-2-phenylindole (DAPI) (Wako; diluted 1:300) for 45 min. To prevent fading, cells were then mounted in DakoCytomation Fluorescent Mounting Medium (DakoCytomation).

### Transfection and luciferase assays

Cells ($8.0\times10^5$) seeded and cultured in 60 mm dishes (Becton Dickinson) were transfected 18 h after plating using Lipofectamine 2000 (Invitrogen) and PLUS reagent (Invitrogen) in Opti-MEM (Gibco). Transfection contained 1.0 μg of TOPflash plasmid (Upstate Biotechnology) for measurement of Wnt/β-catenin activity, or 5.0 μg of the *Id1* promoter-Lux plasmid (provided by Dr Imamura and Dr Miyazono) for measurement of BMP-induced *Id1* gene transcription, and 0.5 μg of pRL-CMV (Promega) as co-transfected control. Medium containing 10% FBS was changed 3 h after transfection and transfected cells ($1.8\times10^5$) were re-seeded in 6-well plates 24 h after transfection. After 18 h, CL6 cells were induced with BMP2 (100 ng/ml) and DMSO. CL6 cells were prepared for luciferase activity analysis using Dual luciferase reporter assay system (Promega).

### Area calculation

The regions of interest (beating area, immunostaining area) were defined in Photoshop (Adobe systems) using the 'magic wand' tool. The total numbers of pixels identified were then counted using the histogram function. At least five different fields were measured for each dish.

### Statistical analysis

Results, shown as the mean±SE, were compared by ANOVA followed by Scheffé's test, with $P<0.05$ considered significant.

## Supporting Information

**Figure S1** A semi-quantitative RT-PCR of cardiomyocyte-specific genes. To investigate expression level of cardiomyocyte-specific genes (Csx/Nkx2.5, Gata4, MyLC-2a, and MyLC-2v), a semi-quantitative RT-PCR was performed from CL6 cells treated with 1% DMSO and the indicated concentration of Grem1 for 14 days. Each RT-PCR product was electrophoresed in 2% agarose gel, and was measured using ImageJ software (http://rsb.info.nih.gov/ij/) to calculate the ratio of each gene to Gapdh. The expression level for each gene is determined relative to that of Gapdh, and expression level in CL6 cells treated with DMSO alone was regarded as 1.0. The relative expression levels were averaged from at least three independent experiments.
Found at: doi:10.1371/journal.pone.0002407.s001 (1.04 MB DOC)

**Figure S2** Grem1 enhanced cardiomyogenic differentiation of mouse ES cells. Mouse ES cells (NCH1.5, C57BL/6J×129ter/Sv) were cultured on a mouse embryonic fibroblast feeder layer inactivated with 30 Gy γ-irradiation in gelatin-coated 60 mm dishes (Becton, Dickinson). Cells were grown in KnockOut DMEM (Gibco) supplemented with 15% fetal bovine serum (Cell Culture Technologies), 2 mM GlutaMAX (Gibco), 0.1 mM non-essential amino acid (Gibco), 0.1 mM 2-mercaptoethanol (Gibco), penicillin, streptomycin, and 2,000 U/ml mouse leukemia inhibitory factor (LIF) (Chemicon). For cardiomyogenic differentiation, ES cells were exposed to 125 ng/ml Grem1 (R&D systems) for the three days. The cells were then trypsinized and cultured to form embryonic bodies (EBs) from a single cell using a three-dimensional culture system (without LIF) on low cell binding dishes (96-well plate round bottom). This represented day 0 of EB formation. On the next day, the medium was replaced with the same medium without LIF. EBs were re-seeded on gelatin-coated 48-well plates with one EB per well, on day 8 after the start of EB formation. The cardiomyogenic induction was estimated by the beating EB number per total EB number, measured on day 12 under a phase-contrast microscope. Grem1 increased the percentage of beating EBs to 69.2%, as compared with 26.7% in EBs without Grem1 treatment. The numbers in parentheses indicate the EB numbers counted.
Found at: doi:10.1371/journal.pone.0002407.s002 (1.27 MB DOC)

**Table S1** Primer sequences.
Found at: doi:10.1371/journal.pone.0002407.s003 (0.06 MB DOC)

**Movie S1** CL6 cells treated with DMSO alone. P19CL6 cells are reproducibly and stably induced into beating cardiomyocytes with DMSO.
Found at: doi:10.1371/journal.pone.0002407.s004 (1.66 MB MOV)

**Movie S2** CL6 cells treated with Grem1 (125 ng/ml) and DMSO. Grem1 dramatically promotes DMSO-induced cardiomyogenic differentiation of P19CL6 cells at a concentration of 125 ng/ml.
Found at: doi:10.1371/journal.pone.0002407.s005 (2.40 MB MOV)

## Acknowledgments

We would like to express our sincere thanks to T. Imamura and K. Miyazono for the *Id1* promoter-Lux plasmid, and J. Fujimoto for their discussion of this work.

## Author Contributions

Conceived and designed the experiments: AU DK. Performed the experiments: DK HM RI KM. Analyzed the data: AU AN DK YT RI MT MW. Contributed reagents/materials/analysis tools: IK AN IS HS. Wrote the paper: AU DK.

## References


1. Andree B, Duprez D, Vorbusch B, Arnold HH, Brand T (1998) BMP-2 induces ectopic expression of cardiac lineage markers and interferes with somite formation in chicken embryos. Mech Dev 70: 119–131.
2. Schultheiss TM, Burch JB, Lassar AB (1997) A role for bone morphogenetic proteins in the induction of cardiac myogenesis. Genes Dev 11: 451–462.
3. Angello JC, Kaestner S, Welikson RE, Buskin JN, Hauschka SD (2006) BMP induction of cardiogenesis in P19 cells requires prior cell-cell interaction(s). Dev Dyn 235: 2122–2133.
4. Alsan BH, Schultheiss TM (2002) Regulation of avian cardiogenesis by Fgf8 signaling. Development 129: 1935–1943.
5. Crossley PH, Martin GR (1995) The mouse Fgf8 gene encodes a family of polypeptides and is expressed in regions that direct outgrowth and patterning in the developing embryo. Development 121: 439–451.
6. Reifers F, Walsh EC, Leger S, Stainier DY, Brand M (2000) Induction and differentiation of the zebrafish heart requires fibroblast growth factor 8 (fgf8/acerebellar). Development 127: 225–235.
7. Whitehead GG, Makino S, Lien CL, Keating MT (2005) fgf20 is essential for initiating zebrafish fin regeneration. Science 310: 1957–1960.
8. Yamagishi H, Olson EN, Srivastava D (2000) The basic helix-loop-helix transcription factor, dHAND, is required for vascular development. J Clin Invest 105: 261–270.
9. Ariizumi T, Kinoshita M, Yokota C, Takano K, Fukuda K, et al. (2003) Amphibian in vitro heart induction: a simple and reliable model for the study of vertebrate cardiac development. Int J Dev Biol 47: 405–410.
10. Gavert N, Ben-Ze'ev A (2007) beta-Catenin signaling in biological control and cancer. J Cell Biochem 102: 820–828.
11. Chien KR, Moretti A, Laugwitz KL (2004) Development. ES cells to the rescue. Science 306: 239–240.
12. Pandur P, Lasche M, Eisenberg LM, Kuhl M (2002) Wnt-11 activation of a non-canonical Wnt signalling pathway is required for cardiogenesis. Nature 418: 636–641.
13. Yamagishi H, Yamagishi C, Nakagawa O, Harvey RP, Olson EN, et al. (2001) The combinatorial activities of Nkx2.5 and dHAND are essential for cardiac ventricle formation. Dev Biol 239: 190–203.
14. Park M, Wu X, Golden K, Axelrod JD, Bodmer R (1996) The wingless signaling pathway is directly involved in Drosophila heart development. Dev Biol 177: 104–116.
15. Marvin MJ, Di Rocco G, Gardiner A, Bush SM, Lassar AB (2001) Inhibition of Wnt activity induces heart formation from posterior mesoderm. Genes Dev 15: 316–327.
16. Schneider VA, Mercola M (2001) Wnt antagonism initiates cardiogenesis in Xenopus laevis. Genes Dev 15: 304–315.
17. Tzahor E, Lassar AB (2001) Wnt signals from the neural tube block ectopic cardiogenesis. Genes Dev 15: 255–260.
18. Olson EN (2001) Development. The path to the heart and the road not taken. Science 291: 2327–2328.
19. Terami H, Hidaka K, Katsumata T, Iio A, Morisaki T (2004) Wnt11 facilitates embryonic stem cell differentiation to Nkx2.5-positive cardiomyocytes. Biochem Biophys Res Commun 325: 968–975.
20. Sharov AA, Dudekula DB, Ko MS (2005) A web-based tool for principal component and significance analysis of microarray data. Bioinformatics 21: 2548–2549.
21. Hamatani T, Carter MG, Sharov AA, Ko MS (2004) Dynamics of global gene expression changes during mouse preimplantation development. Dev Cell 6: 117–131.
22. Sharov AA, Dudekula DB, Ko MSH (2005) http://lgsun.grc.nia.nih.gov/ANOVA/help.html#hierarchical Accessed 2007 April 20. Bioinformatics Advance Access.
23. Naito AT, Akazawa H, Takano H, Minamino T, Nagai T, et al. (2005) Phosphatidylinositol 3-kinase-Akt pathway plays a critical role in early cardiomyogenesis by regulating canonical Wnt signaling. Circ Res 97: 144–151.
24. Hsu DR, Economides AN, Wang X, Eimon PM, Harland RM (1998) The Xenopus dorsalizing factor Gremlin identifies a novel family of secreted proteins that antagonize BMP activities. Mol Cell 1: 673–683.
25. Naito AT, Shiojima I, Akazawa H, Hidaka K, Morisaki T, et al. (2006) Developmental stage-specific biphasic roles of Wnt/beta-catenin signaling in cardiomyogenesis and hematopoiesis. Proc Natl Acad Sci U S A 103: 19812–19817.
26. Jin EJ, Erickson CA, Takada S, Burrus LW (2001) Wnt and BMP signaling govern lineage segregation of melanocytes in the avian embryo. Dev Biol 233: 22–37.
27. Sutherland MK, Geoghegan JC, Yu C, Turcott E, Skonier JE, et al. (2004) Sclerostin promotes the apoptosis of human osteoblastic cells: a novel regulation of bone formation. Bone 35: 828–835.
28. Shi W, Zhao J, Anderson KD, Warburton D (2001) Gremlin negatively modulates BMP-4 induction of embryonic mouse lung branching morphogenesis. Am J Physiol Lung Cell Mol Physiol 280: L1030–1039.
29. Tzahor E, Kempf H, Mootoosamy RC, Poon AC, Abzhanov A, et al. (2003) Antagonists of Wnt and BMP signaling promote the formation of vertebrate head muscle. Genes Dev 17: 3087–3099.
30. Zuniga A, Michos O, Spitz F, Haramis AP, Panman L, et al. (2004) Mouse limb deformity mutations disrupt a global control region within the large regulatory landscape required for Gremlin expression. Genes Dev 18: 1553–1564.
31. Michos O, Panman L, Vintersten K, Beier K, Zeller R, et al. (2004) Gremlin-mediated BMP antagonism induces the epithelial-mesenchymal feedback signaling controlling metanephric kidney and limb organogenesis. Development 131: 3401–3410.
32. Yuasa S, Itabashi Y, Koshimizu U, Tanaka T, Sugimura K, et al. (2005) Transient inhibition of BMP signaling by Noggin induces cardiomyocyte differentiation of mouse embryonic stem cells. Nat Biotechnol 23: 607–611.
33. Singh JP, Chaikin MA, Pledger WJ, Scher CD, Stiles CD (1983) Persistence of the mitogenic response to platelet-derived growth factor (competence) does not reflect a long-term interaction between the growth factor and the target cell. J Cell Biol 96: 1497–1502.
34. Frank NY, Kho AT, Schatton T, Murphy GF, Molloy MJ, et al. (2006) Regulation of myogenic progenitor proliferation in human fetal skeletal muscle by BMP4 and its antagonist Gremlin. J Cell Biol 175: 99–110.
35. Klaus A, Saga Y, Taketo MM, Tzahor E, Birchmeier W (2007) Distinct roles of Wnt/beta-catenin and Bmp signaling during early cardiogenesis. Proc Natl Acad Sci U S A 104: 18531–18536.
36. Yamaguchi TP, Takada S, Yoshikawa Y, Wu N, McMahon AP (1999) T (Brachyury) is a direct target of Wnt3a during paraxial mesoderm specification. Genes Dev 13: 3185–3190.
37. Kleber M, Lee HY, Wurdak H, Buchstaller J, Riccomagno MM, et al. (2005) Neural crest stem cell maintenance by combinatorial Wnt and BMP signaling. J Cell Biol 169: 309–320.
38. Sugiki T, Uyama T, Toyoda M, Morioka H, Kume S, et al. (2007) Hyaline cartilage formation and enchondral ossification modeled with KUM5 and OP9 chondroblasts. J Cell Biochem 100: 1240–1254.

# Nicotine Acts on Growth Plate Chondrocytes to Delay Skeletal Growth through the α7 Neuronal Nicotinic Acetylcholine Receptor

**Atsuo Kawakita[1,2], Kazuki Sato[2], Hatsune Makino[1], Hiroyasu Ikegami[2], Shinichiro Takayama[3], Yoshiaki Toyama[2], Akihiro Umezawa[1]***

1 Department of Reproductive Biology, National Institute for Child Health and Development, Tokyo, Japan, 2 Department of Orthopaedic Surgery, Keio University School of Medicine, Tokyo, Japan, 3 Department of Orthopaedic Surgery, National Center for Child Health and Development, Tokyo, Japan

## Abstract

***Background:*** Cigarette smoking adversely affects endochondral ossification during the course of skeletal growth. Among a plethora of cigarette chemicals, nicotine is one of the primary candidate compounds responsible for the cause of smoking-induced delayed skeletal growth. However, the possible mechanism of delayed skeletal growth caused by nicotine remains unclarified. In the last decade, localization of neuronal nicotinic acetylcholine receptor (nAChR), a specific receptor of nicotine, has been widely detected in non-excitable cells. Therefore, we hypothesized that nicotine affect growth plate chondrocytes directly and specifically through nAChR to delay skeletal growth.

***Methodology/Principal Findings:*** We investigated the effect of nicotine on human growth plate chondrocytes, a major component of endochondral ossification. The chondrocytes were derived from extra human fingers. Nicotine inhibited matrix synthesis and hypertrophic differentiation in human growth plate chondrocytes in suspension culture in a concentration-dependent manner. Both human and murine growth plate chondrocytes expressed alpha7 nAChR, which constitutes functional homopentameric receptors. Methyllycaconitine (MLA), a specific antagonist of alpha7 nAChR, reversed the inhibition of matrix synthesis and functional calcium signal by nicotine in human growth plate chondrocytes in vitro. To study the effect of nicotine on growth plate in vivo, ovulation-controlled pregnant alpha7 nAChR +/− mice were given drinking water with or without nicotine during pregnancy, and skeletal growth of their fetuses was observed. Maternal nicotine exposure resulted in delayed skeletal growth of alpha7 nAChR +/+ fetuses but not in alpha7 nAChR −/− fetuses, implying that skeletal growth retardation by nicotine is specifically mediated via fetal alpha7 nAChR.

***Conclusions/Significance:*** These results suggest that nicotine, from cigarette smoking, acts directly on growth plate chondrocytes to decrease matrix synthesis, suppress hypertrophic differentiation via alpha7 nAChR, leading to delayed skeletal growth.

**Citation:** Kawakita A, Sato K, Makino H, Ikegami H, Takayama S, et al. (2008) Nicotine Acts on Growth Plate Chondrocytes to Delay Skeletal Growth through the α7 Neuronal Nicotinic Acetylcholine Receptor. PLoS ONE 3(12): e3945. doi:10.1371/journal.pone.0003945

**Editor:** Rory Edward Morty, University of Giessen Lung Center, Germany

**Received** August 6, 2008; **Accepted** November 8, 2008; **Published** December 16, 2008



**Funding:** This study was supported by a grant from the Smoking Research Foundation; by grants from the Ministry of Education, Culture, Sports, Science, and Technology (MEXT) of Japan; by the Ministry of Health, Labour and Welfare (MHLW) Sciences Research Grants; by a Research Grant on Health Science focusing on Drug Innovation from the Japan Health Science Foundation; by the program for promotion of Fundamental Studies in Health Science of the Pharmaceuticals and Medical Devices Agency; by a Research Grant for Cardiovascular Disease from the MHLW; and by a Grant for Child Health and Development from the MHLW. The funders had no role in study design, data collection and analysis, decision to publish, or preparation of the manuscript.

**Competing Interests:** The authors have declared that no competing interests exist.

* E-mail: umezawa@1985.jukuin.keio.ac.jp

## Introduction

Though detrimental effects of cigarette smoking to the human body have been widely demonstrated, the effects on endochondral ossification are not well understood. Epidemiologically, maternal smoking reduces the height of newborns [1–5]. However, there are controversial views regarding the mechanisms behind delayed skeletal growth caused by cigarette smoking. The socioeconomic status of smoking mothers [6,7], deficient maternal diet [8], chronic hypoxia caused by carbon monoxide [9], impaired placental size and function, and decreased blood flow of placenta caused by nicotine [10] have all been reported as a possible causal factors responsible for reduction in height of newborns. Conversely, it has also been reported that socioeconomic status [11], maternal diet [12], and hypoxia are not responsible for the cause of delayed skeletal growth. Research suggests that smoking not only reduces body length but also brings ossification retardation in the rat smoking model [13]. Moreover, smoking delays chondrogenesis in a mouse model of fracture healing [14]. Cigarette smoking, thus, adversely affects endochondral ossification somehow during the course of skeletal growth and repair in animal models.

Among a multitude of chemicals and physiological functions arising from cigarette smoking, nicotine is one of the leading candidates for causing small newborns. Epidemiologically, nicotine content in cigarette is related to reduced birth length in humans [15]. However, the possible mechanism of delayed skeletal growth caused by nicotine remains unclarified. In this study, we investigated the effect of nicotine on growth plate chondrocytes, the principle

component of endochondral ossification. In the last decade, localization of neuronal nicotinic acetylcholine receptor (nAChR), a specific receptor of nicotine, has been widely detected in non-excitable cells [16]. Therefore, we hypothesized that nicotine affect growth plate chondrocytes directly and specifically through nAChR to delay skeletal growth. We here demonstrate that nicotine affected growth plate chondrocytes through alpha7 nAChR to decrease matrix synthesis and to suppress hypertrophic differentiation, thereby delaying skeletal growth.

## Results

### Detection and localization of nAChR in growth plate chondrocytes

To date, many epidemiological [1–5] and experimental [13] studies suggested that endochondral ossification is affected by cigarette smoking, especially by its major component, nicotine [15]. We thus assumed that nicotine may directly affect chondrocytes, a key player in endochondral ossification. To investigate whether the impact of nicotine on chondrocytes is specific, we studied the expression pattern of the specific receptor, nAChR. For screening of the existing subunits of nAChR, RT-PCR was performed with primers for each subunit of nAChR. Human growth plate chondrocytes expressed alpha5, alpha7, beta1 and epsilon subunits of nAChR (Figure 1A).

Among the detected subunits, only the alpha7 subunit can form a functional nAChR by forming a homopentameric receptor [17]. We thus tried to detect alpha7 subunit at a protein level. Western blot analysis revealed that chondrocytes produced alpha7 nAChR (Figure 1B). Immunocytochemical analysis also revealed that chondrocytes stained positive for alpha7 nAChR (Figure 1C). Moreover, the alpha7 subunit was detected at resting, proliferating and pre-hypertrophic chondrocytes of murine growth plate but not hypertrophic chondrocytes (Figure 1D). These results suggest that the growth plate chondrocytes in their non-hypertrophic stage express alpha7 homopentameric nAChR.

### Effect of nicotine on chondrocytes cultured in agarose gel

To study the effect of nicotine on growth plate chondrocytes in vitro, two methods of suspension cultures, i.e., agarose gel culture and alginate bead culture, were employed. In agarose gel, the chondrocytes are initially embedded in the suspension layer solitarily. The chondrocytes then proliferate, differentiate, and aggregate to form a colony in the presence of ascorbic acid, and start to produce a matrix around themselves [18]. We applied the agarose gel culture to study the effect of nicotine on the proliferation and differentiation of growth plate chondrocytes in vitro. Nicotine was added to culture media for three weeks culture period. Nicotine decreased the percentage of colonies which produce matrix, as revealed by alcian blue (ALB) stains in a concentration-dependent manner (Figure 2A, upper panels). Similarly, nicotine suppressed Col X expression and enzyme activity of alkaline phosphatase (ALP) in a concentration-dependent manner (Figure 2A, middle and lower row panels). In contrast, nicotine did not affect colony density (Figure 2B, left panel) or the number of cells per colony (Figure 2B, right panel) which are indicators for cell proliferation. No nicotinic effect on cell proliferation was detected as assessed by immunohistochemistry using antibody to proliferating cell nuclear antigen (PCNA) (Figure S1). These results suggest that nicotine decreases the matrix synthesis and suppresses hypertrophic differentiation of growth plate chondrocytes, but has little effect on cell proliferation in vitro and vivo. To investigate if the nicotinic effect is mediated by alpha7 nAChR, we used MLA, the specific antagonist of alpha7 nAChR. MLA clearly reversed the effect, as assessed by ALB-stained colonies (Figure 2C), suggesting the involvement of alpha7 nAChR in the effect of nicotine on growth plate chondrocytes.

### Long-term (four months) effect of nicotine on growth plate chondrocytes in alginate beads

Different from the case with agarose gel, human chondrocytes hardly proliferate in alginate beads, maintaining chondrocyte properties for more than eight months [19]. Moreover, molecular analysis can be done easily compared with that in agarose gel, since chondrocytes can be recovered from beads by chelation of divalent ions with ethylenediamine tetraacetic acid (EDTA) followed by centrifugation. We investigated the long-term effect of nicotine on growth plate chondrocytes by employing alginate bead culture. Chondrocytes encapsulated in alginate beads remained viable during the culture period (four months) in their lacunae. Nicotine did not affect viability of the chondrocytes at any indicated concentration. Nicotine dose-dependently suppressed ALB- and Safranin-O-stained areas at four months (Figure 3A).

To investigate expression of chondrocyte-specific genes, we performed RT-PCR analysis on chondrocytes in alginate beads. Genes for collagen type II (Col II), Aggrecan, collagen type X (ColX), ALP, and indian hedgehog (Ihh) were up-regulated at three weeks after the start of alginate bead culture (Figure 3B). In contrast, genes for parathyroid hormone receptor type I (PTHR1), matrix metalloproteinase type 13 (MMP13), vascular endothelial growth factor (VEGF), and Sox9 were constitutionally expressed and their expression level remained unchanged. We then performed RT-PCR analysis to investigate the expression of chondrocyte-specific genes in chondrocytes treated by nicotine for four months. Nicotine dose-dependently decreased the expression of Col II, Aggrecan, Col X, ALP, and Ihh gene (Figure 3C). These findings suggest that nicotine suppresses matrix synthesis and hypertrophic maturation of chondrocytes in long-term culture using alginate beads.

### Functional calcium imaging

To investigate the intracellular signals after nicotinic stimulation, we performed calcium imaging assay for primary chondrocyte cultures, since alpha7 nAChR has large $Ca^{2+}$ permeabilities and also induces elevated intracellular free calcium by releasing intracellular calcium stores [17]. Nicotine elicited a transient increase of intra-cellular calcium (Figure 4A) in a concentration-dependent manner (Figure 4B). MLA, the specific antagonist of alpha7 nAChR, inhibited the calcium signals in a concentration-dependent manner (Figure 4C), implying that the effect of nicotine on chondrocytes is mediated through the alpha7 nAChR.

### Maternal nicotine exposure in wild-type mice

To study the effect of nicotine on endochondral ossification in vivo, ovulation-controlled pregnant C57BL/6J mice were given drinking water with or without nicotine during pregnancy, and skeletal growth of their fetuses was observed. At noon on gestational day 15, fetuses were surgicallly obtained and their legs were sectioned for measurement of the femur length (FL) and the length of the hypertrophic zone of the femur (HL) (Figure 5A). There were no significant differences of the amount of water consumed between nicotine-exposed group and control group. Maternal nicotine exposure significantly reduced the FL (Figure 5B) and HL/FL (Figure 5C) of mice at embryonic day 15.5 (E15.5), suggesting that nicotine delayed endochondral ossification.

### Maternal nicotine exposure in alpha7 nAChR-disrupted mice

To clarify an involvement of alpha7 nAChR in nicotine-induced delayed skeletal growth in vivo, we investigated the effect

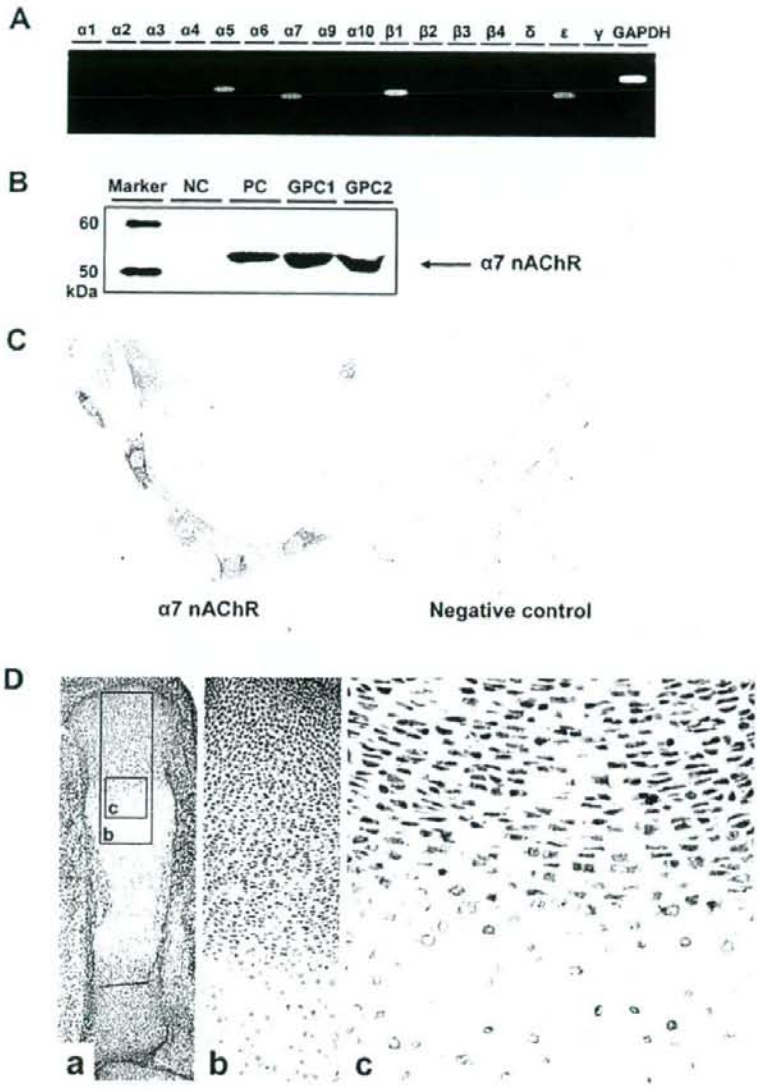


**Figure 1. Detection and localization of nAChR subunits in growth plate chondrocytes.** A: The expression of each subunit of nAChR. Total RNA was isolated from primary culture of human growth plate chondrocytes. The primers for each subunit are listed in Tables S1–S3. RT-PCR amplified products of alpha5, alpha7, beta1 and epsilon subunits of nAChR and GAPDH. B: Western blot analysis of alpha7 subunit of nAChR in primary chondrocyte cultures. NC: negative control (adipocyte), PC: positive control (PC-12 cell), GPC1,2: human growth plate chondrocyte derived from extra fingers of two individuals. C: Immunocytochemical analysis of alpha7 nAChR subunit in human growth plate chondrocytes. Primary chondrocytes were stained with alpha7 nAChR subunit-specific antibody. D: Immunohistochemical analysis of alpha7 nAChR subunit in tibia of E15.5 fetuses. Alpha7 nAChR are detected at resting, proliferating and pre-hypertrophic chondrocytes of murine growth plate.
doi:10.1371/journal.pone.0003945.g001

of maternal nicotine exposure on skeletal development of murine fetuses in which the alpha7 nAChR gene is disrupted. Maternal genotype is alpha7 nAChR +/− in this experiment (Figure 6), unlike the experiment using wild type mice (Figure 5, maternal genotype: alpha7 nAChR +/+), and littermate fetuses (alpha7 nAChR −/− and alpha7 nAChR +/+) were compared to exclude the effect of nicotine on maternal bodies. Nicotine significantly reduced FL and HL/FL in alpha7 nAChR +/+ fetuses but not in alpha7 nAChR −/− fetuses (Figure 6A, B). However, nicotine did not significantly affect body weight (BW) in both genotypes

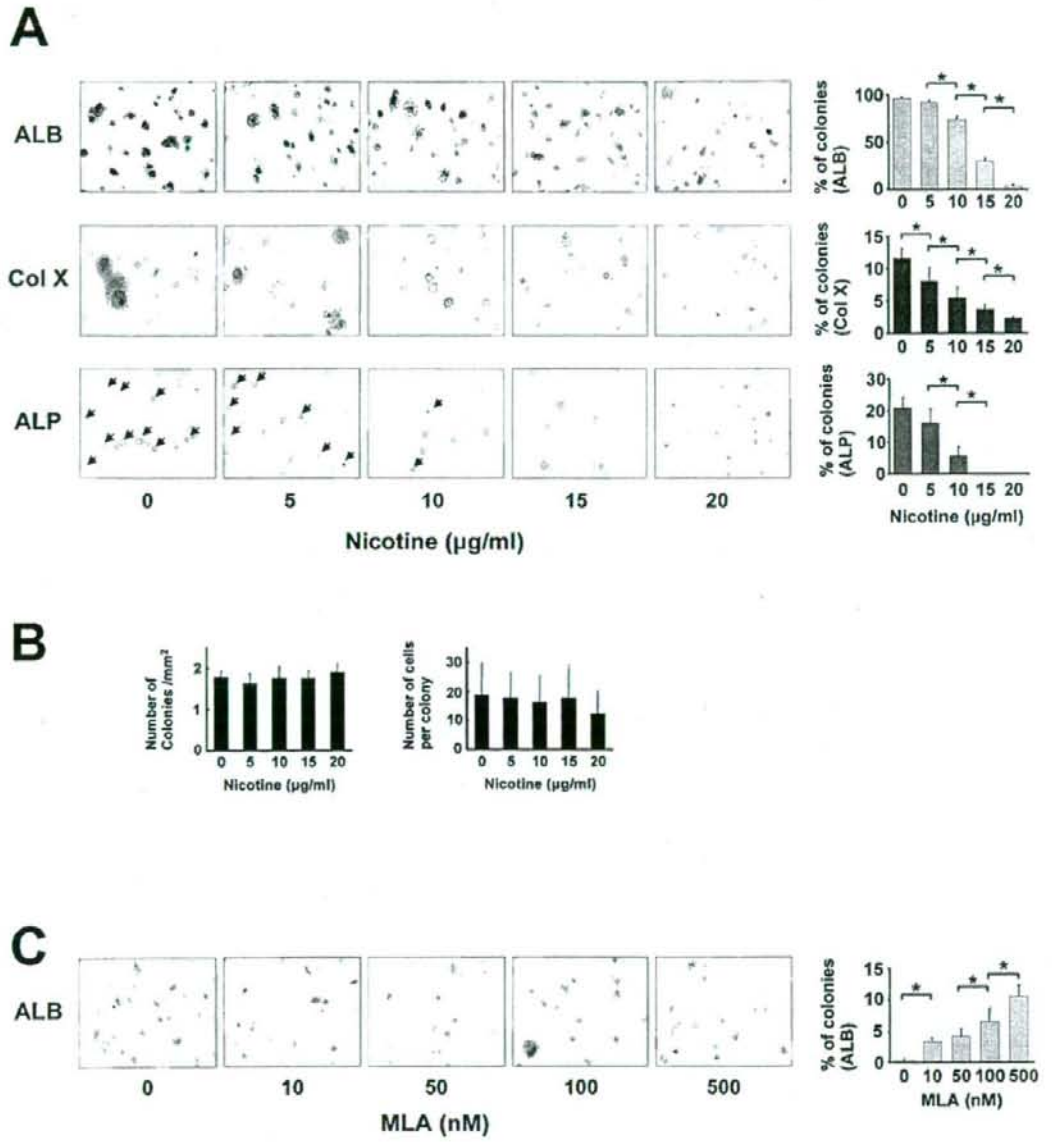


**Figure 2. Effect of nicotine on growth plate chondrocytes in agarose gel.** Growth plate chondrocytes were cultured in an agarose gel using the modified method previously described [28], and exposed to nicotine and MLA, a specific antagonist for alpha7 nAChR, at the indicated concentration. After three weeks of cultivation, suspension agarose was transferred to a glass slide and the following histological analyses were then performed. A: Microscopic appearance of chondrocyte colonies. From top to bottom: ALB (Alcian blue stain), Col X (immunocytochemistry by an anti-Col X antibody), ALP (enzyme cytochemistry of alkaline phosphatase). For ALB and Col X stain, the slides were counterstained with kernechtrot and hematoxylin, respectively. Percentage of ALB- stained, Col X- positive, and Alkaline phosphatase- positive colonies were counted (right panel, from top to bottom). All the ALP positive colonies in the panels are indicated by arrowheads. Nicotine concentration-dependently suppressed the percentage of the colonies stained with ALB, Col X, and ALP. *, statistically significant, $P<0.02$. B: Number of colonies and number of cells per colony. The number of colonies with a diameter greater than 50 μm (left panel) and cell number per colony (right panel) were counted on the ALB- stained agarose gel slides. C: Microscopic appearance of chondrocyte colonies stained with ALB. MLA reversed the decrease of ALB- positive matrix in a concentration-dependent manner under constant nicotine concentration (20 μg/ml). The percentage of ALB-positive colonies exceeded 10% by using 500 nM MLA. *, statistically significant, $P<0.02$.

doi:10.1371/journal.pone.0003945.g002